DEVELOPMENT OF A STEWART PLATFORM MANIPULATOR

by

MANJUNATH HEGDE

DEPARTMENT OF MECHANICAL ENGINEERING

INDIAN INSTITUTE OF TECHNOLOGY KANPUR

APRIL, 1993

DEVELOPMENT OF A STEWART PLATFORM MANIPULATOR

A Thesis Submitted
in Partial Fulfilment of the Requirements
for the Degree of
MASTER OF TECHNOLOGY

by

MANJUNATH HEGDE

to the

DEPARTMENT OF MECHANICAL ENGINEERING
INDIAN INSTITUTE OF TECHNOLOGY KANPUR
APRIL, 1993

DEDICATED

TO

MY PARENTS -

CERTIFICATE

This is to certify that the present work DEVELOPMENT OF A STEWART PLATFORM MANIPULATOR by Manjunath Hegde has been carried out under our supervision and that it has not been submitted elsewhere for a degree.

Prof. A. K. Mallik
Head, Center for Robotics
I. I. T. Kanpur

Dr. S. Mukherjee
Asst. Prof. Mechanical Engg.
I. I. T. Kanpur

ACKNOWLEDGEMENTS

I feel fortunate to have worked with Prof. A. K. Mallik and Dr. S. Mukherjee. They were the source of direction and help, all along my association with them. I am thankful to both of them for the guidance they provided to me, at every stage of my thesis.

I wish to thank Mr. R. M. Jha, Mr. Prem Prakesh and all others in Manufacturing Sc. Lab who helped me in realizing the Stewart Platform Manipulator.

I am also thankful to Mr. S. Sen and other friends of Robotics Center who took great pains in designing the controller for the manipulator.

I extend my thanks to Mr. Rakesh Bairathi, Mr. Rajiv Tiwari and Mr. Soumya Bhattacharya for useful discussions with them during the course of this work.

My thanks are also due to Amiya, Anirvan, Dwivedi, Telang and other friends who made my stay at I. I. T. a pleasure.

MANJUNATH HEGDE

CONTENTS

CONTENTS

NOMENCLATURE

$[\,]^T$	column matrix
$[n, s, a]$	3 X 3 combined rotation matrix
T	4 X 4 transformation matrix
i	suffix, 1 to 3
J	suffix, 1 to 6
J	rotary inertia Kg m^2
J	jacobian matrix
K_1, K_2	constants
Li	length of i^{th} upper link mm
Di	length of i^{th} lower link mm
δ	half-stroke mm
lmean, dmean	mean length of upper, lower link mm
M	mass Kg
P, P^*	pitch m/radian
α	acceleration m sec^{-2}
τ	torque N m
r, r'	actual, apparent radius of platform mm
R	support-structure radius mm
θ	joint rotation
ϕ_i, ξ_i	constant angles
_lsb, _usb	upper support bar, lower support bar
_spp, _hg	SPM, hinge
w, p	world coordinate, platform coordinate

LIST OF FIGURES

ABSTRACT

Stewart Platform Manipulator (SPM) is a six degrees-of-freedom parallel manipulator proposed by D. Stewart [1965].

An SPM, owing to its parallel architecture, has high rigidity and hence better suited for the heavy duty applications. Singular configurations and poor workspace are its major drawbacks.

In the present work the position kinematics of an SPM has been considered in detail. This study has been extended to motion simulation and workspace analysis of the manipulator. Various link parameters have been derived to arrive at a design.

The kinematic design considerations of the manipulator, emphasizing the link interferences and manipulator compactness have been presented. An SPM conforming to the above mentioned studies and analysis has been fabricated. The present design employing lead-screw based actuators can be well suited in the applications needing high precision and accuracy.

CHAPTER 1

INTRODUCTION

1.1 INTRODUCTION

Stewart Platform Manipulator (SPM), specifically robots with parallel architecture has special bearing on research aimed at developing manipulators for heavy duty applications. Robotic manipulators generally fall under following three classes based on the arrangement of actuators.

(a) Serial manipulators

(b) Parallel manipulators

(c) Hybrid systems

Most robot arms, whether in industrial robots or other manipulators have their actuators connected in series along a more or less anthropomorphic arm. Each actuator is either at or associated with single degree-of-freedom [Fig. 1.1(a)]. These serial type manipulator with an open kinematic chains have some drawbacks. The most important one being high elastic flexibility due to the cantilever type of links (arms). To overcome these structure-inherent shortcomings, researchers have proposed closed kinematic chain, generally called parallel chains.

A fully parallel manipulator [Fig. 1.1(c)] generally has all its actuators connected directly to the end effector. Here several constraints simultaneously determine the relationship of one body to another. Unlike serial manipulators, these possess higher stiffness, better dynamic characteristics and hence are better suited to heavy duty applications. However, its reachable work area is small and kinematic analysis is comparatively

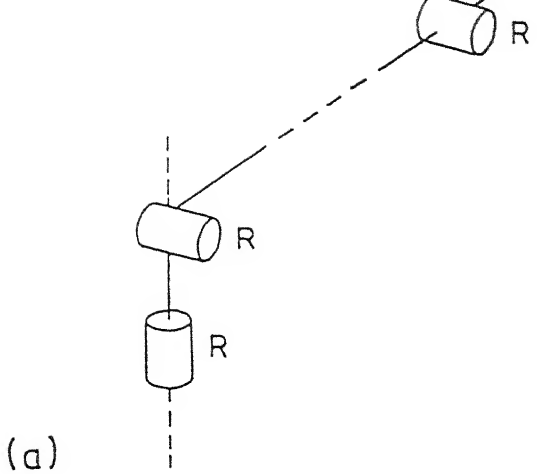

(a)

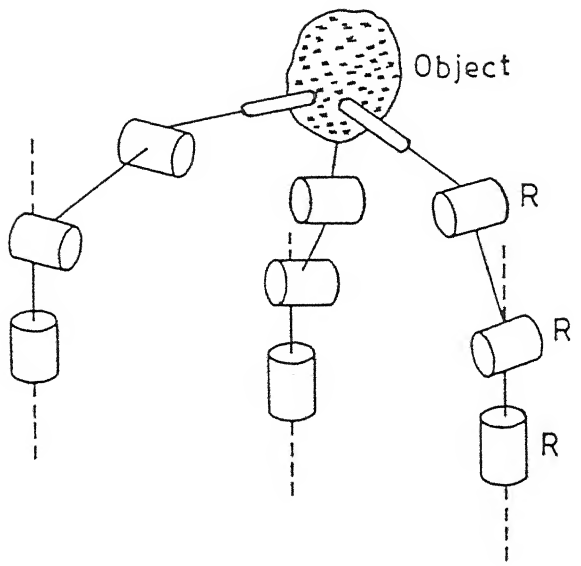

(b)

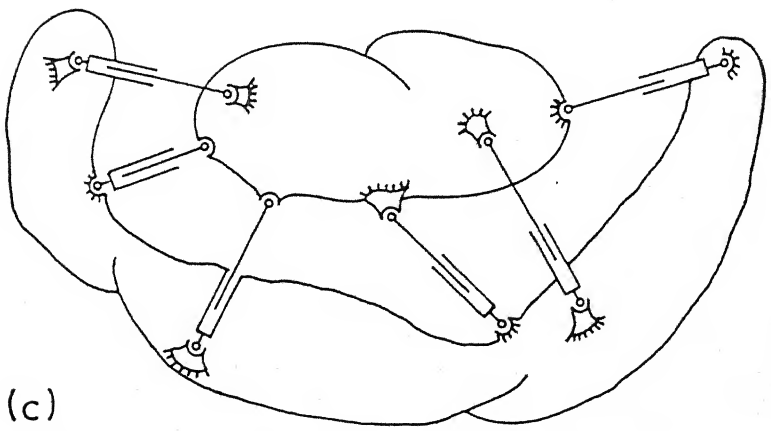

(c)

Fig. 1.1. A schematic sketch showing (a) serial, (b) hybrid system and (c) parallel manipulators.

complicated. Additionally the number of special configurations or singularities in the workspace is far more than that for a serial manipulator.

As opposed to fully serial or parallel arrangement of actuators, it is possible to have structures which have serial as well as parallel actuation. Such manipulators come under hybrid system [Fig. 1.1(b)]. Multiple coordinated manipulators, walking vehicles and multifingered grippers belong to this class of mechanisms. These manipulators can have good workspace and maneuverability as compared to a parallel manipulator, also, better rigidity and dynamic performance in comparison to serial chain manipulators.

1.2 STEWART PLATFORM TYPE MANIPULATORS

These are all parallel manipulators generally referred to as in-parallel actuated manipulators, general stewart platform manipulator etc.

Most general six degrees-of-freedom manipulators have been shown in Figs. 1.2(a) and 1.2(b). In both the cases, a top and bottom plates are connected by six length controllable linear actuators. Both the mechanisms make use of spherical joints. The workspace and maneuverability are poor.

Parallel manipulators with three degrees-of-freedom have been shown in Figs. 1.3(a) and 1.3(b), the former one is planar parallel manipulator, the latter one is spherical manipulator. In the planar type, joints are revolute and the three motors M1, M2, M3 are fixed. This manipulator has only planar movements. The spherical manipulator, which consists of

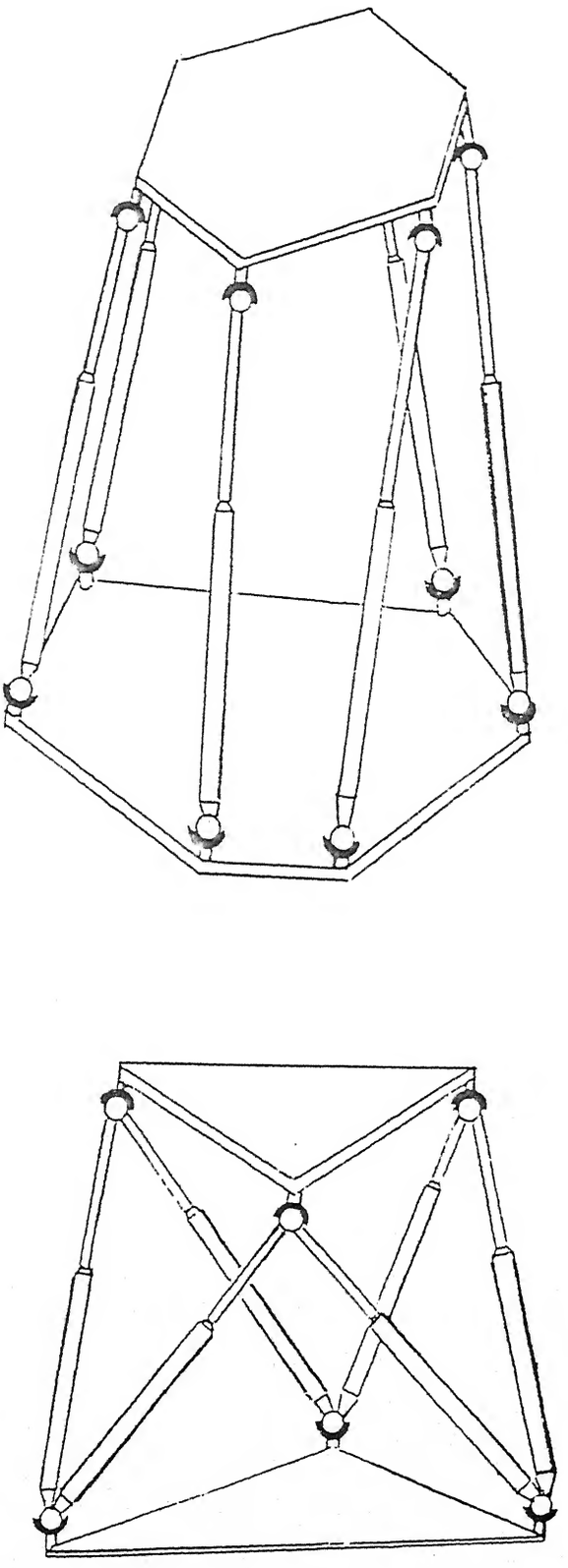

Fig. 1.2 General six degrees-of-freedom parallel manipulators.

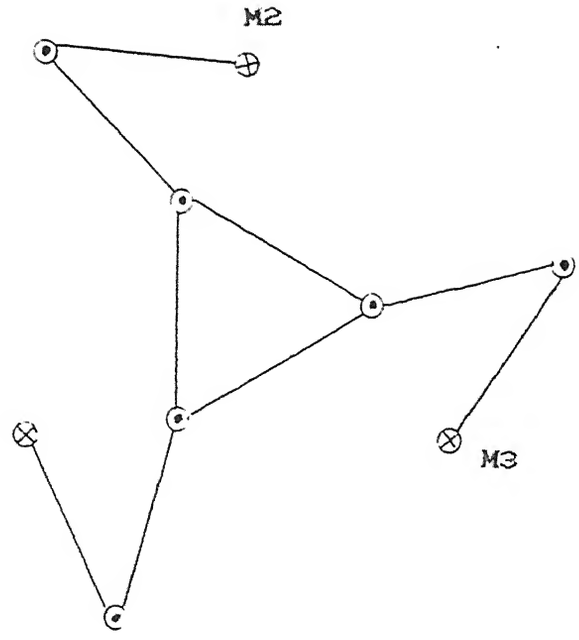

(a)

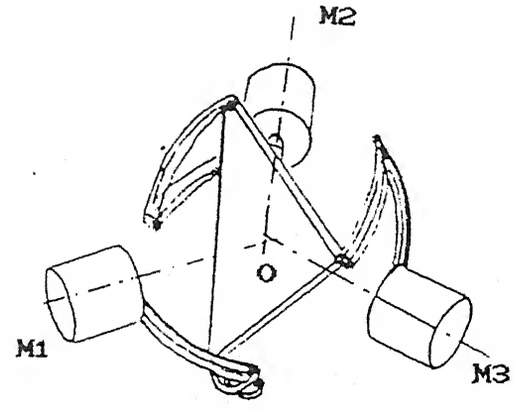

(b)

Fig. 1.3 Three degrees-of-freedom manipulators

(a) Planar type

(b) Spherical type.

three motors M1, M2 and M3, with axes passing through a common point (O as shown in Fig. 1.3(b)), has only rotational degrees-of-freedom.

1.3 STEWART PLATFORM MANIPULATOR

D. Stewart [1965] proposed an eight bar spatial mechanism for simulating flight conditions [Fig. 1.4], which is generally referred to by latter researchers as the Stewart Platform Manipulator. This mechanism, as shown, consists of a triangular plate (platform), six length controllable linear actuators and a rigid foundation. Two actuators in pair constitute a leg of the manipulator and hence an SPM has three legs. Each leg is connected to one of the corners of the platform through a ball-and-socket type joint (spherical joint). The connection between the foundation and a leg is through a two-axis (two degrees-of-freedom) joint. Thus, the mechanism consists of three spherical joints and three two-axis joints.

If point p is the point of attachment of one of the leg systems to the platform, its motion can be decomposed into two basic modes. The lines of the two actuators define a plane. The actuator motions specify the motions of point P in the above plane completely. Motion of point P out of the plane is not directly specified by the two actuators as it is free to spin about the axis SS'. Its motion is, however, constrained by the geometry of the rest of the platform.

This mechanism, as suggested by D. Stewart, has following applications :

(a) As a vehicle for representing a body in space subjected to

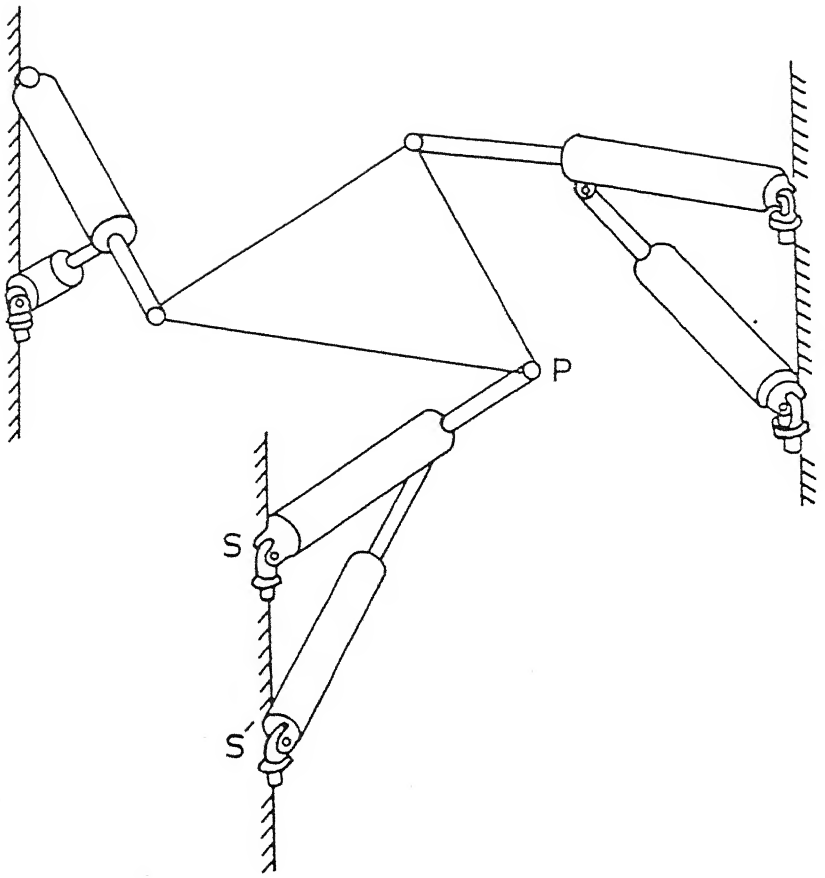

Fig. 1.4. A pictorial view of Stewart platform manipulator .

all the forces which may be encountered in its voyage.

(b) As representing a platform held stationary in space mounted on a vessel such as a ship which is subjected to the random movements of the sea.

(c) As a platform for simulating the actions of the helicopter as driven by its pilot or

(d) As a support for a helicopter which is capable of being driven by the pilot, random actions being applied to the supporting platform as prescribed.

(e) As any vehicle which is subjected to control by a human being.

(f) As a basis of design for a new form of machine tool.

(g) As a basis of design for an automatic assembly or transfer machine.

1.4 LITERATURE REVIEW

D. Stewart [1] was the first to propose a parallel manipulator for flight simulation. The above paper also gives an account of various control arrangements, strength considerations etc. Since then, researchers have proposed a large variety of arrangements, of which a few have been mentioned in section 1.2.

Hirochika Inoue [2] developed a parallel manipulator which is similar to an eight bar spatial linkage SPM. The method of actuation here, is by three sets of pantograph link mechanisms, each of which is driven by a pair of DC motors instead of linear actuators.

Yang and Lee [3] presented an analysis of a six degrees-of-freedom Stewart platform [Fig. 1.2 (a)] which include the synthesis of platform type structures for functioning as

robotic positioners, displacement analysis, physical constraint investigation, analysis of workspace and maneuverability of the mechanism.

Design of planar three degrees-of-freedom parallel mechanism [Fig. 1.3 (a)] has been considered by Gosselin and Angles [4], emphasizing non vanishing workspace criterion and symmetry. Gosselin and Angles [5] also presented the planning of trajectory for three degrees-of-freedom parallel manipulators using jacobian based condition number as an optimality index. Gosselin [6] provided a workspace generating algorithm for a six degrees-of-freedom parallel manipulator [Fig. 1.2 (a)]. The reachable workspace, dexterous workspace and the controllably dexterous workspace have been studied by Kumar [11].

Hunt [7] has presented the synthetic methods for determining assembly configurations of in-parallel-actuated manipulators and analogies between serial and parallel devices.

The direct kinematics of some special form of Stewart platform manipulators have been studied by Nanua [8], Lin [9] and Parenti-Castelli [10].

1.5 PRESENT STUDY

The present work aims at developing a manipulator with six degrees-of-freedom, based on Stewart mechanism. This, we will refer to as Stewart Platform Manipulator or SPM.

The problem of position kinematics for the manipulator has been studied in detail. Inverse kinematics has been used in the workspace analysis of the manipulator and in deriving various manipulator dimensions. A simulation of the mechanism has been developed using 3D graphics. The simulation in conjunctiom

with numerical solution of the direct kinematics problem has been used to analyze the interference effects and workspace of the manipulator.

A systematic approach has been used in formulating various design considerations, evolving link parameters, achieving compactness of the manipulator and ensuring interference free movements.

A Stewart Platform Manipulator has been developed conforming to above studies, analysis and simulation.

Chapters 2 and 3 have been devoted for analyzing the position kinematics problem of an SPM. The predesign simulation has been presented in chapter 3. The various design considerations of the manipulator have been discussed in chapter 4. Chapter 5 concludes the present study.

CHAPTER 2

KINEMATIC ANALYSIS AND CONTROL EQUATIONS

A schematic arrangement of the Stewart Platform Manipulator (SPM) is shown in Fig. 2.1.

The design consists of a triangular flat plate called platform which is supported by three leg systems. Each leg system consists of two linear actuators, the Upper Linear Actuator (ULA) and the Lower Linear Actuator (LLA). Each ULA has one end connected by a spherical (S-joint) joint to the platform corner and the other end to the foundation (support) through a two-axis joint (RR-joint). Each LLA has its one end connected to a ULA through a revolute (R-joint) joint while other end to the support through an RR-joint. The LLA controls the angle of the ULA with respect to the support. The plane containing the ULA and LLA can rotate about a common vertical axis passing through the centres of upper and lower RR-joints.

2.1 NUMBER SYNTHESIS

A general form of the degrees-of-freedom equation for both planar and spatial mechanism can be written as follows :

$$F = \lambda (n - j - 1) + \sum_{i=1}^{j} fi + fd \qquad (2.1)$$

where

F = resulting degrees-of-freedom,

λ = the degrees-of-freedom of space in which the mechanism operates,

n = number of links,

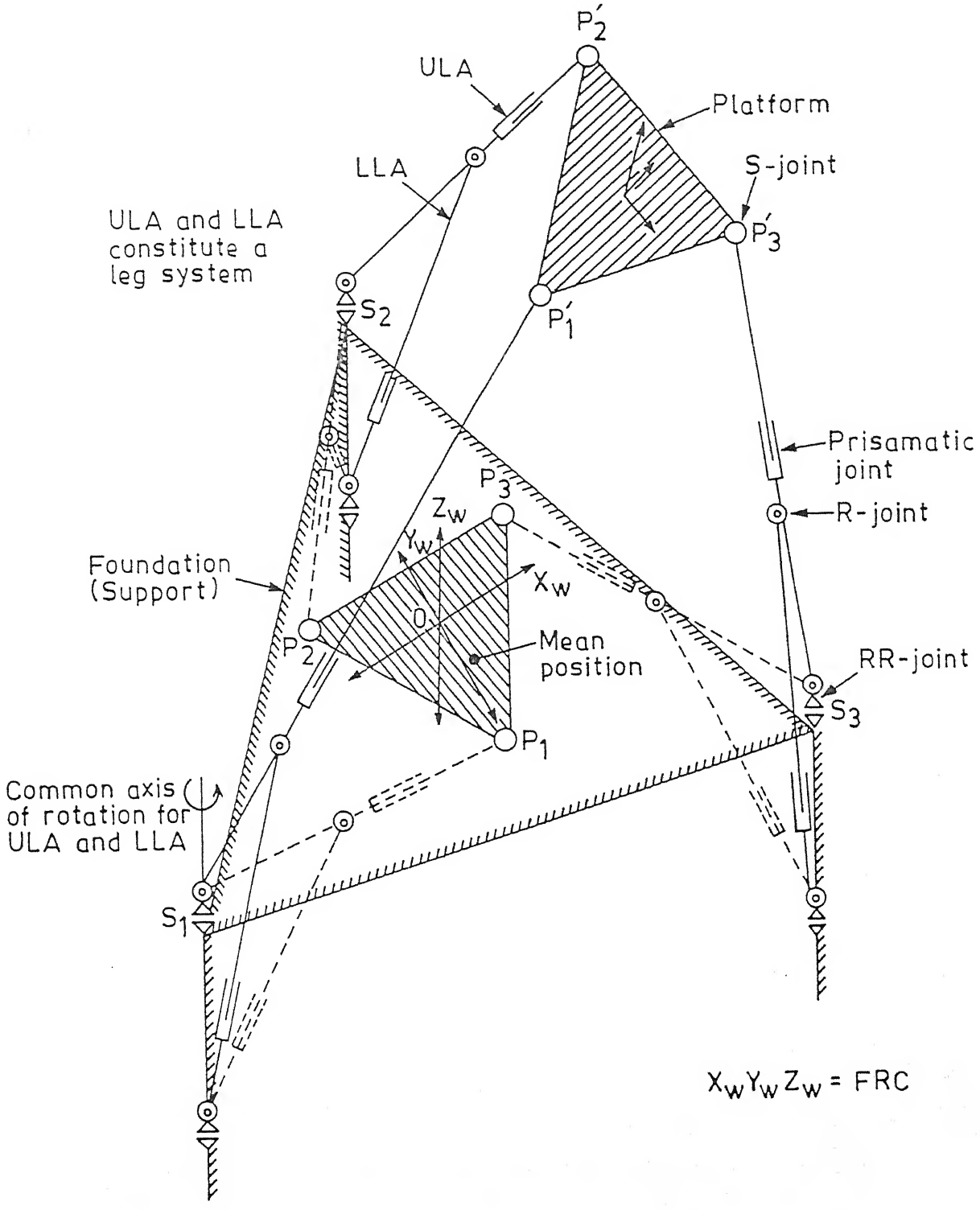

Fig. 2.1. Mechanism for SPM.

j = number of joints.

fi = degrees-of-freedom of i^{th} joint and

fd = idle or passive degrees-of-freedom.

Referring to Fig. 2.1, it has three spherical joints, three prismatic joints and three RR-joints. Therefore, from (2.1) we can write

$$F(\text{active}) = 6(5 - 6 - 1) + (2 \times 3 + 1 \times 3 + 3 \times 3) + 0 = 6.$$

$$F(\text{locked}) = 6(5 - 6 - 1) + (1 \times 3 + 0 \times 3 + 3 \times 3) + 0 = 0.$$

Thus, SPM is a structure for a given position of the actuators but it has six degrees-of-freedom when the joints are active. Hence an SPM allows six controllable degrees-of-freedom.

2.2 MECHANICAL ELEMENTS OF SPM

An SPM, like other spatial mechanisms, consists of links (viz., actuator, platform, support), joints and drives [see Fig. 1.4].

2.2.1 ACTUATOR

Actuator used is of lead-screw type [Fig. 2.2]. A DC Servomotor rigidly fixed to an L-support rotates a lead-screw mounted between the other two L-supports. The angle sections supporting the lead-screw are provided with bush bearings. The nut sliding on a polished base plate transmits linear motion to the support bar. All the six actuators are identical.

The support bar, rigidly fixed to the nut, is an intgeral part of the actuator. The free end of the upper support bar has been connected to a corner of the platform through an S-joint and

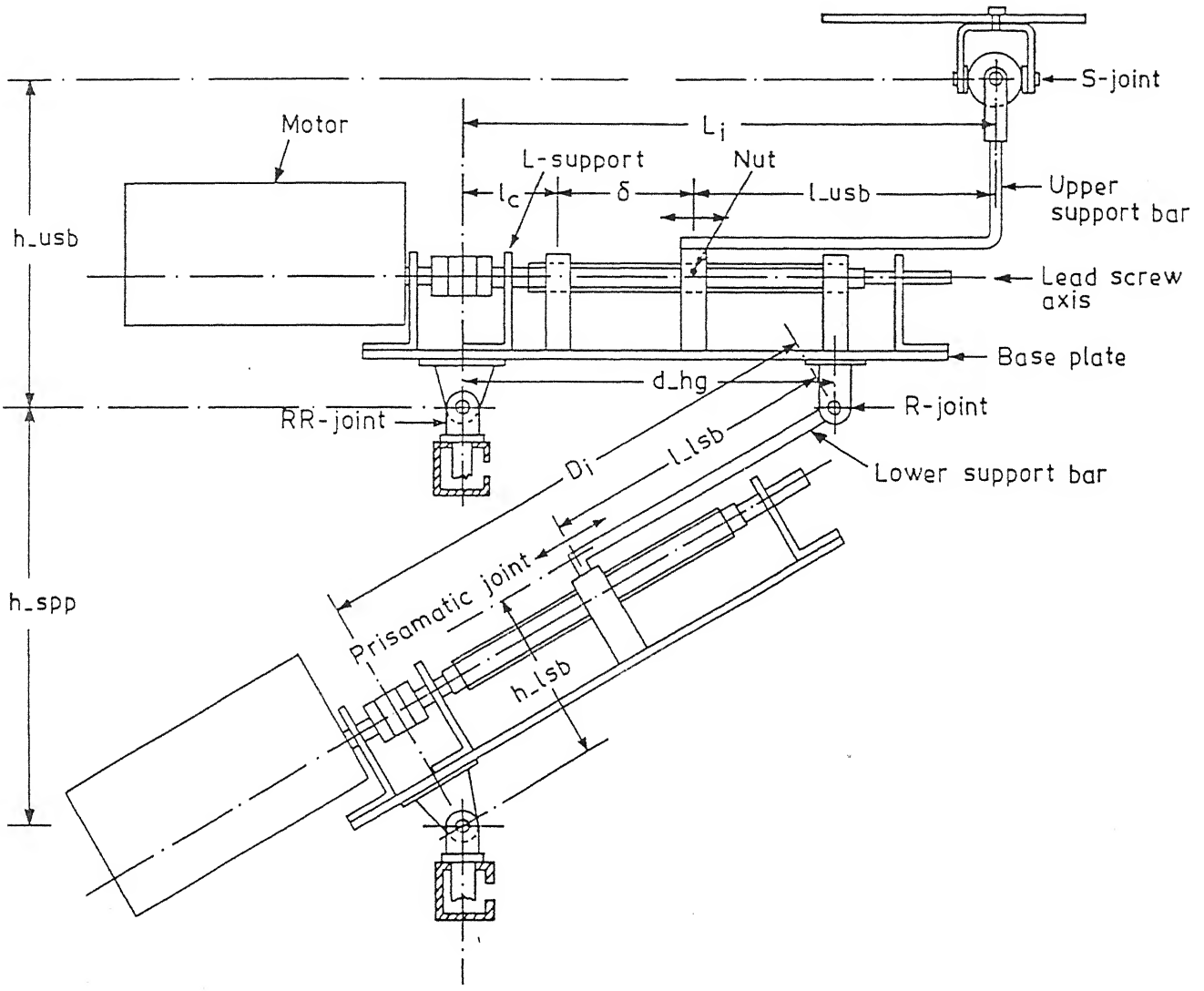

Fig. 2.2. General arrangement of leg system showing design and control parameters of SPM.

that of the lower support bar is connected to the base plate of the lower actuator through an R-joint.

The combination of an actuator and the support bar constitutes a link of the manipulator. There are three such upper links which have been referred to as the Upper Linear Actuator (ULA). Each upper link has corresponding lower link called the Lower Linear Actuator (LLA).

DC Servomotors are used as the drive part of each actuator. They have inherent advantage of possessing good power to weight ratio, high efficiency, speed independent torque and inbuilt position feedback.

Lead-screw based actuators, inspite of high frictional losses, have advantages as listed below :

* Simplicity of construction, design
* Smooth and noiseless
* High load carrying capacity
* Self locking
* High accuracy of motion

2.2.2 PLATFORM

Platform is the physical end effector of an SPM [see Fig. 2.3]. This is a plate, one of the three corners of which is connected through an S-joint to seperate leg systems. Since the platform has three support points, it has been referred to as triangular. This has been designed as an equilateral triangle for symmetry. The same reasoning applies for taking six identical actuators, equilateral support structure points etc.

The size of the platform refers to its size contained

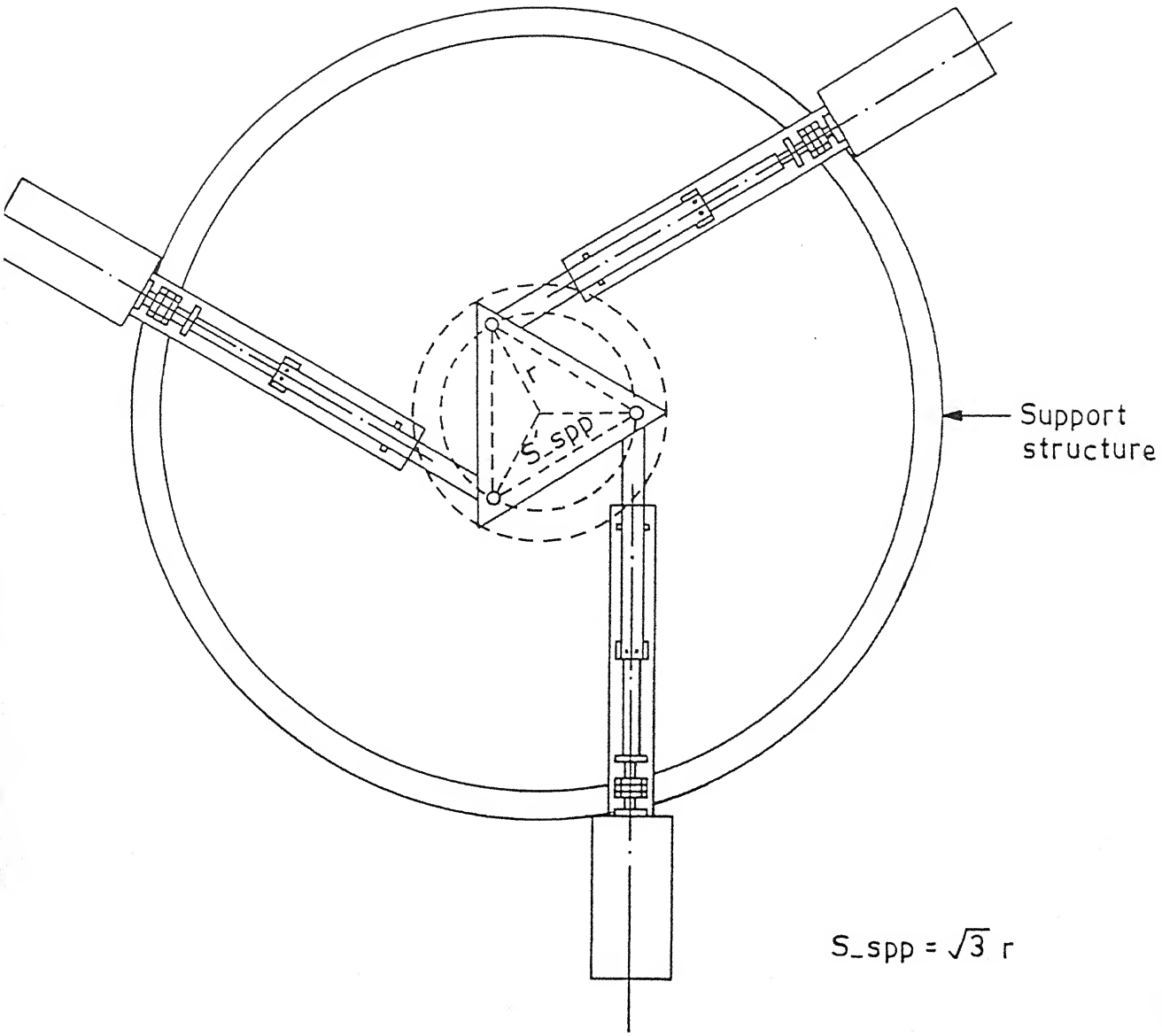

Fig. 2.3. Top view of SPM.

between centers of three S-joints.

2.2.3 SUPPORT STRUCTURE

This is a rigid support made up of two support rings [Fig. 2.3], the upper and the lower, connected by three vertical legs at 120° spacing. The upper support ring supports ULA and the lower support ring supports LLA, in a manner such that the upper and the lower RR-joints have common vertical axis of revolution.

Practically, a support structure represents a rigid foundation whose design should be compact, besides it should not interfere with the actuator movements.

2.2.4 JOINTS

These serve as connections between two or more links. However, in the present design of SPM only lower pairs constitute a connection between two kinematic links. These have been classified on the basis of degrees-of-freedom they possess and or the nature of motion they transmit to the adjoining link [Fig. 2.2].

A lead-screw and nut constitute a single degree-of-freedom screw pair.

The connection between the base plate of ULA and the free end of the lower support bar is a Revolute joint (R-joint). The axis of freedom of this joint is parallel to the base plate and normal to the lead-screw axis.

Two-axis joints or RR-joints connect the base plate of ULA and LLA to the upper and lower support rings, respectively. This

joint has two degrees-of-freedom, namely, the rotations

(i) about an axis normal to the ground and passing through the centre of the joint and

(ii) about an axis parallel to the R-joint axis and passing through the centre of the joint.

The latter one is controlled by the LLA, while the former one determined by the constraints within the mechanism.

Spherical joint (S-joint) is a three-degrees-of freedom ball and socket joint, which theoretically transmits no torque but force. The present design employs a three-axis universal type joint (Hooke's joint type) as shown in Fig.2.2. It connects the corner of the platform to the free end of the upper support bar. This joint can rotate about

(i) an axis normal to the plane of the platform and passing through the center of the joint,

(ii) an axis parallel to the plane of the platform and passing through the center of the joint and

(iii) an axis normal to above two and passing through the center of the joint.

2.3 KINEMATIC CHAINS AND THEIR PARAMETERS

Series of links connected by kinematic pairs constitute a kinematic chain. A leg system, which is formed by three links, the ULA, LLA and the support structure, is a simple closed chain [Fig. 2.2]. Since the support structure is a fixed link, a leg system with its joints locked can be considered as a structure which can rotate about the common vertical axis of upper and lower RR-joints. Further, any two leg systems along with the

support structure and platform as other two links form a four-link closed chain [Fig. 2.3], which gives rise to more than one assembly configurations of SPM.

Various parameters of an SPM leg system which will be referred to in the analysis, design and control have been illustrated in Fig. 2.2.

Upper actuator length (Li) is defined as the distance of the center of S-joint from the center of upper RR-joint, measured parallel to the upper lead-screw axis [see Fig.2.2]. Length of LLA (Di) is the distance between the R-joint center and the center of lower RR-joint. The notations for the displacements of nut from its mean position are δ_{Li} and δ_{Di}.

The angles θ_{1i} and θ_{2i}, respectively, represent the rotations of RR-joint about its horzontal and vertical axes of freedom.

2.4 ANALYSIS OF GEOMETRY

This section aims at developing kinematic equations for an SPM, which is the basis for analysis and control of motions of the manipulator.

2.4.1 MEAN POSITION

An SPM is defined to be in its mean position iff

(i) The platform is parallel to the ground and

(ii) a line drawn parallel to lead-screw axis of ULA, passing through the center of S-joint is parallel to the ground and perpendicular to the median of the platform triangle passing through that particular S-joint.

In other words, at the mean position of the platform, all ULA's are tangential to the circle containing the platform. [see Fig. 2.3]

A coordinate system fixed as at the mean position, as shown in Fig. 2.4, has been taken as the World Coordinate system (WC) and the same has been referred to as the Fixed Reference Coordinate system (FRC). This particaluar position (mean position) represents the center of work space of a symmetric SPM.

The present symmetric design ensures the mean position of the platform is attained when all the six actuators are in their respective mean position. This implies the following relations :

$\delta_{Li} = 0,$

$\delta_{Di} = 0,$

the mean length of ULA (l_mean) $= l_c + \delta + l_{usb}$,

the mean length of LLA (d_mean) $= l_c + \delta + l_{lsb}$, (2.2)

where

δ = half stroke of the actuator,

l_c = dead length of the actuator (minimum position of the nut),

l_{usb}, l_{lsb} = lengths of upper and lower support bars [Fig.2.2].

Li = l_{mean}

Di = d_{mean}

To track the position and orientation of the platform with respect to FRC, one more coordinate system called Platform Fixed Coordinate system (PFC) or moving coordinate system has been

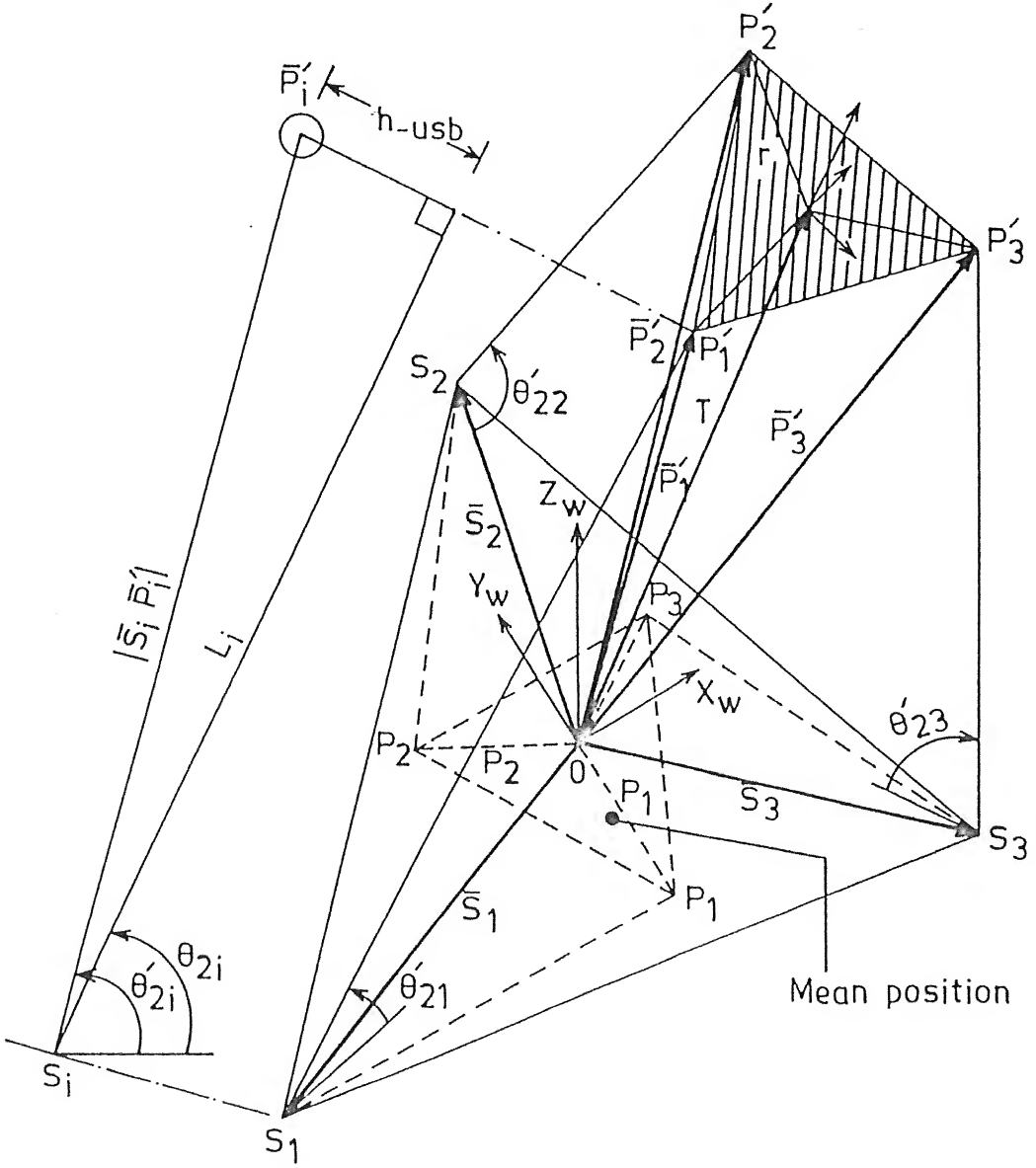

$|\bar{S}_i| = R$

$\bar{S}_i$ = Position vectors of support points

$\bar{P}'_i$ = Position vectors of platform points

$|\bar{P}_i| = r$

$\bar{P}_i$ = Position vectors of platform points at its mean position

$$|\bar{S}_i \bar{P}'_i|^2 = L_i^2 + h_{-usb}^2$$

$$\theta_{2i} = \theta'_{2i} - \sin^{-1}\left[\frac{h_{-usb}}{|\bar{S}_i \bar{P}'_i|}\right]$$

Fig. 2.4. Inverse kinematic parameters of SPM.

attached to the platform. Unlike FRC which is fixed in space, PFC has been attached to the geometric center of the platform and moves along with the platform. From Fig. 2.4, it is evident that PFC coincides with FRC when the platform is at the mean position.

2.4.2 INVERSE POSITION KINEMATICS

This refers to the computations of the actuator lengths, as a function of the given position and orientation of the platform.

Referring to Fig. 2.4, the position vectors of all points will be referred to FRC only, and the position and orientation of platform will imply position and orientation of PFC with respect to FRC.

Let $\bar{S}_i$ be the position vector of the center of the upper RR-joints and $\bar{P}_i$ be the position vector of the corner of the platform in its mean position. If the platform moves to a new position and orientation given by the following [4 X 4] transformation matrix T,

$$T = \begin{bmatrix} n_x & s_x & a_x & x_p \\ n_y & s_y & a_y & y_p \\ n_z & s_z & a_z & z_p \\ 0 & 0 & 0 & 1 \end{bmatrix} \qquad (2.3)$$

then, the new position of the platform corner say $\bar{P}_i'$ is given by following equation :

$$\begin{bmatrix} \bar{P}_i' \\ 1 \end{bmatrix} = T \begin{bmatrix} \bar{P}_i \\ 1 \end{bmatrix} \qquad (2.4)$$

The length of the upper actuator corrosponds to $|\bar{P}_i' - \bar{S}_i'|$, and the inclination of the upper actuator to the foundation can be

computed by considering the displacement of the platform corner in Z direction.

Referring to Figs. 2.2 and 2.4,

$$\bar{S1} = [\ -l_{mean},\ -r,\ -h_{usb}\ ]^T$$

$$\bar{S2} = \left[\ \left(\frac{l_{mean}}{2} - \frac{\sqrt{3}}{2} r\right), \left(\frac{\sqrt{3}}{2} l_{mean} + \frac{r}{2}\right),\ -h_{usb}\right]^T$$

$$\bar{S3} = \left[\ \left(\frac{l_{mean}}{2} - \frac{\sqrt{3}}{2} r\right), \left(-\frac{\sqrt{3}}{2} l_{mean} + \frac{r}{2}\right),\ -h_{usb}\ \right]^T$$

$$\bar{P1} = [\ 0,\ -r,\ 0\ ]^T$$

$$\bar{P2} = \left[-\frac{\sqrt{3}}{2} r,\ \frac{r}{2},\ 0\ \right]^T$$

$$\bar{P3} = \left[\ \frac{\sqrt{3}}{2} r,\ \frac{r}{2},\ 0\ \right]^T$$

Using the above relation in (2.4) we get

$$\begin{bmatrix} \bar{P}_1' \\ 1 \end{bmatrix} = T \begin{bmatrix} \bar{P}_1 \\ 1 \end{bmatrix}$$

$$= \begin{bmatrix} x_p + r\left(-s_x\right) \\ y_p + r\left(-s_y\right) \\ z_p + r\left(-s_z\right) \\ 1 \end{bmatrix},$$

Similarly,

$$\begin{bmatrix} \bar{P}_2' \\ 1 \end{bmatrix} = T \begin{bmatrix} \bar{P}_2 \\ 1 \end{bmatrix}$$

$$= \begin{bmatrix} x_p + \frac{r}{2}\left(-\sqrt{3}\, n_x + s_x\right) \\ y_p + \frac{r}{2}\left(-\sqrt{3}\, n_y + s_y\right) \\ z_p + \frac{r}{2}\left(-\sqrt{3}\, n_z + s_z\right) \\ 1 \end{bmatrix}.$$

and

$$\begin{bmatrix} \bar{P}_3' \\ 1 \end{bmatrix} = T \begin{bmatrix} \bar{P}_3 \\ 1 \end{bmatrix}$$

$$= \begin{bmatrix} x_p + \frac{r}{2}\left(\sqrt{3}\, n_x + s_x\right) \\ y_p + \frac{r}{2}\left(\sqrt{3}\, n_y + s_y\right) \\ z_p + \frac{r}{2}\left(\sqrt{3}\, n_z + s_z\right) \\ 1 \end{bmatrix}.$$

Referring to Fig.2.4, we use the following symbols :

Li = length of ULA,

Di = length of LLA,

θ_{2i} = Inclination of ULA to a horizontal plane,

h_usb = height of the S-joint (as shown) a constant,

and r = radius of the platform circle.

Referring to Fig.2.4, θ_{2i}' represent the inclination of the line joining the center of S-joint and the support point to a horizontal plane.

Since the actuator lengths have been measured parallel to the lead-screw axis, we can write

$$Li = \sqrt{|\bar{P}_i - \bar{S}_i|^2 - (h\_usb)^2} \qquad (2.5)$$

$$\theta_{2i}' = \sin^{-1}\left\{ \frac{\text{height of } i^{th} \text{ corner from the support point}}{|\,\bar{P}_i' - \bar{S}_i\,|} \right\}$$

$$\theta_{2i} = \theta_{2i}' - \sin^{-1}\left\{ \frac{h\_usb}{|\,\bar{P}_i' - \bar{S}_i\,|} \right\} \qquad (2.6)$$

For i = 1, 2, 3, the above expressions simplify to the following form :

$$L1 = \sqrt{l\_mean^2 + 2\, l\_mean\, X_1 + 2\, h\_usb\, Z_1 + X_1^2 + Y_1^2 + Z_1^2}$$

$$L2 = \sqrt{l\_mean^2 - l\_mean\, X_2 - \sqrt{3}\, l\_mean\, Y_2 + 2\, h\_usb\, Z_2 + X_2^2 + Y_2^2 + Z_2^2}$$

$$L3 = \sqrt{l\_mean^2 - l\_mean\, X_3 + \sqrt{3}\, l\_mean\, Y_3 + 2\, h\_usb\, Z_3 + X_3^2 + Y_3^2 + Z_3^2}$$

(2.7)

$$\theta_{21} = \sin^{-1}\left\{ \frac{Z_1 + h\_usb}{\sqrt{L1^2 + h\_usb^2}} \right\} - \sin^{-1}\left\{ \frac{h\_usb}{\sqrt{L1^2 + h\_usb^2}} \right\}$$

$$\theta_{22} = \sin^{-1}\left\{ \frac{Z_2 + h\_usb}{\sqrt{L2^2 + h\_usb^2}} \right\} - \sin^{-1}\left\{ \frac{h\_usb}{\sqrt{L2^2 + h\_usb^2}} \right\}$$

$$\theta_{23} = \sin^{-1}\left\{ \frac{Z_3 + h\_usb}{\sqrt{L3^2 + h\_usb^2}} \right\} - \sin^{-1}\left\{ \frac{h\_usb}{\sqrt{L3^2 + h\_usb^2}} \right\}$$

$X_i = x_p + fx_i,$

$Y_i = y_p + fy_i,$

$Z_i = z_p + fz_i,$

for i = 1, 2, 3. (2.8)

where

$$fx_1 = -r\,s_x,$$

$$fy_1 = -r\,(s_y - 1),$$

$$fz_1 = -r\,s_z,$$

$$fx_2 = \frac{r}{2}\left(-\sqrt{3}\,n_x + s_x + \sqrt{3}\right),$$

$$fy_2 = \frac{r}{2}\left(-\sqrt{3}\,n_y + s_y - 1\right),$$

$$fz_2 = \frac{r}{2}\left(-\sqrt{3}\,n_z + s_z\right),$$

$$fx_3 = \frac{r}{2}\left(\sqrt{3}\,n_x + s_x - \sqrt{3}\right),$$

$$fy_3 = \frac{r}{2}\left(\sqrt{3}\,n_y + s_y - 1\right) \quad \text{and}$$

$$fz_3 = \frac{r}{2}\left(\sqrt{3}\,n_z + s_z\right).$$

(2.9)

Using the experessions for θ_{2i}, the length of LLA can be computed as given below.

Referring to Fig. 2.2, let

h_{spp} be the height of spm, i.e., the vertical distance measured between the centers of the upper and lower RR-joints,

d_{hg} be the distance between the centers of R-joint and RR-joint, measured parallel to lead screw axis,

h_{lsb} be the height of the lower support bar, measured between the center of lower RR-joint and the central axis of lower support bar. The length of LLA can be seen as

$$Di = \sqrt{K_1 + K_2 \sin\theta_{2i}}$$

$$K_1 = h\_spp^2 + d\_hg^2 - h\_leb^2,$$

$$K_2 = 2\, h\_spp\, d\_hg,$$

for i = 1, 2, 3. (2.10)

The lengths of LLA are given by

$$D1 = \sqrt{K_1 + K_2 \sin \theta_{21}}$$

$$D2 = \sqrt{K_1 + K_2 \sin \theta_{22}}$$

$$D3 = \sqrt{K_1 + K_2 \sin \theta_{23}} \quad . \qquad (2.11)$$

The displacements of actuator for a given position and orientation of the platform will follow from

$$\delta_{Li} = Li - lmean$$

$$\delta_{Di} = Di - dmean.$$

(2.12)

As a specific example, using the angle convention shown in Fig. 2.5 where α, β, and γ, respectively, represent the yaw, pitch and roll motions of the platform, the corresponding fx_i, fy_i and fz_i values are obtained as

$$fx_1 = r \left(\cos \alpha \sin \gamma - \sin \alpha \sin \beta \cos \gamma \right),$$

$$fy_1 = r \left(1 - \sin \alpha \sin \beta \sin \gamma - \cos \alpha \cos \gamma \right),$$

$$fz_1 = - r \sin \alpha \cos \beta ,$$

$$fx_2 = \frac{r}{2}\left(-\sqrt{3} \cos \beta \cos \gamma + \sin \alpha \sin \beta \cos \gamma - \sin \gamma \cos \alpha + \sqrt{3}\right),$$

$$fy_2 = \frac{r}{2}\left(-\sqrt{3} \sin \gamma \cos \beta + \cos \alpha \cos \gamma + \sin \alpha \sin \beta \sin \gamma - 1\right),$$

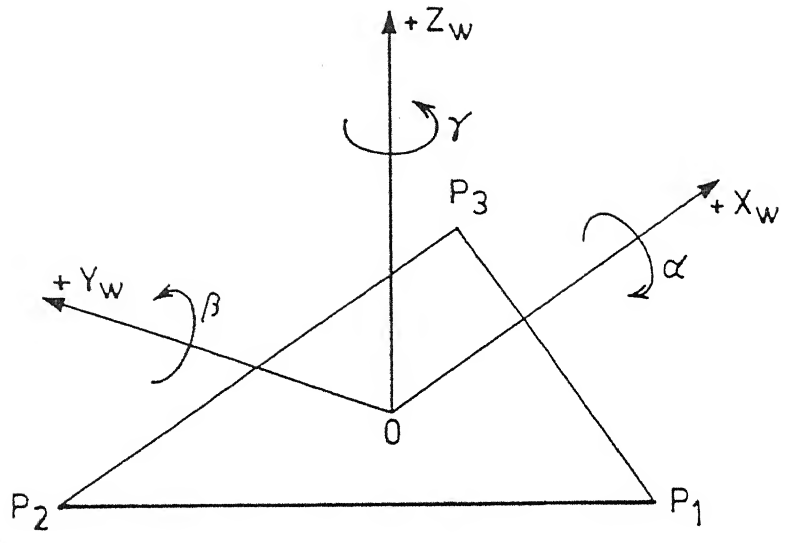

Fig. 2.5. Angle convention – Roll, Pitch and Yaw.

$$fz_2 = \frac{r}{2}\left[\sqrt{3}\sin\beta + \sin\alpha\cos\beta\right],$$

$$fx_3 = \frac{r}{2}\left[\sqrt{3}\cos\beta\cos\gamma - \sin\gamma\cos\alpha + \sin\alpha\sin\beta\cos\gamma - \sqrt{3}\right],$$

$$fy_3 = \frac{r}{2}\left[\sqrt{3}\sin\gamma\cos\beta + \cos\alpha\cos\gamma + \sin\alpha\sin\beta\sin\gamma - 1\right],$$

$$fz_3 = \frac{r}{2}\left[-\sqrt{3}\sin\beta + \sin\alpha\cos\beta\right].$$

(2.13)

Substitution of fx_i, fy_i and fz_i from (2.9) or (2.13), into equations (2.7) and (2.11) gives, respectively, the ULA and LLA lengths.

CHAPTER 3

DIRECT POSITION KINEMATICS

For parallel manipulators like an SPM, the problem of finding the position and orientation of the platform-fixed coordinates with respect to the fixed reference coordinate system, given the set of six actuator lengths,is called the direct position kinematics problem. The inverse kinematic problem of an SPM is straightforward as is the direct position kinematics problem of a serial manipulator. The direct position kinematics of a parallel mechanism and the inverse position kinematics of a serial manipulator are significantly difficult. Recently Roth and Raghavan [1990] have shown that the inverse kinematics problem of a general six degrees-of-freedom serial chain has 16 solutions. The direct kinematic problem of the general stewart platform [Fig. 1.2(a)] is yet unsolved in closed form. But some special cases like the configuration considered here are solvable.

3.1 DIRECT POSITION KINEMATICS IN CLOSED FORM

3.1.1 FORMULATION OF PLATFORM MATRIX

A schematic sketch of the leg system of an SPM has been shown in Fig. 3.1. The following three variables are being introduced :

Li the length of i^{th} ULA,

Di the length of i^{th} LLA,

θ_{1i} is the angle between the positive X_w direction and the i^{th}

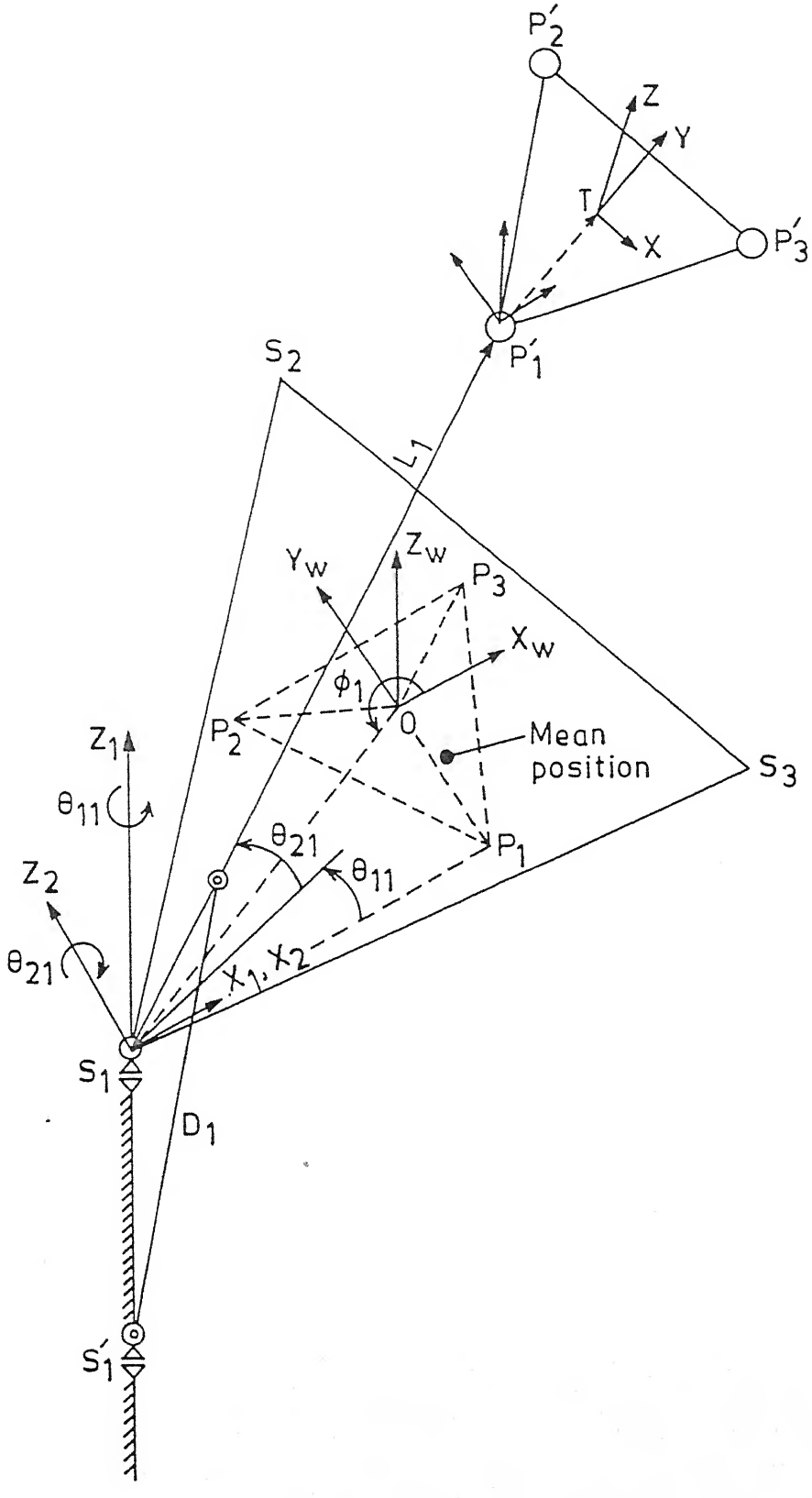

Fig. 3.1. Direct kinematic parameters of SPM.

ULA measured in the XY plane (CCW positive),

θ_{2i} is the angle between the horizontal plane and the i^{th} ULA measured in the XZ plane (CCW positive).

The height of the upper support bar has been neglected, i.e. $h_{usb} = 0$.

The position vector of the i^{th} corner of the platform in the Fixed Reference Coordinate, $\bar{P}_i'$, is given by,

$$\bar{P}_i' = \begin{bmatrix} Li \cos\theta_{2i} \cos\theta_{1i} + R\cos\phi_i \\ Li \cos\theta_{2i} \sin\theta_{1i} + R\sin\phi_i \\ Li \sin\theta_{2i} \end{bmatrix} \qquad (3.1)$$

where,

R = radius of the support ring and

ϕ_i = a constant angle between the positive direction of X_w axis and the line joining the center of the platform at mean position to the center of the RR-joint, when

$$\phi_1 = \phi + \pi$$

$$\phi_2 = \phi + \frac{\pi}{3}$$

$$\phi_3 = \phi - \frac{\pi}{3}$$

where $\phi = \tan^{-1}\left(\frac{r}{l_{mean}}\right)$

with $l_{mean} = \sqrt{R^2 - r^2}$, (3.1.1)

r being the platform circle radius.

For a given LLA length, the angles θ_{2i} are given by the following equation

$$\theta_{2i} = \sin^{-1}\left[\frac{Di^2 - K_1}{k_2}\right]$$

where

$K_1 = h\_spp^2 + d\_hg^2 - h\_lsb^2$,

$K_2 = 2\ h\_spp\ d\_hg$,

[see Fig. 2.2]

for i = 1, 2, 3. (3.1.2)

Hence, for a given set of ULA and LLA lengths, the standard homogeneous end effector (platform) matrix T can be formed as follows:

$$T = \begin{bmatrix} \underset{\sim}{n} & \underset{\sim}{s} & \underset{\sim}{a} & \underset{\sim}{p} \\ 0 & 0 & 0 & 1 \end{bmatrix}$$

where

$$\underset{\sim}{n} = \frac{\bar{P}_2' - \bar{P}_3'}{\sqrt{3}\ r},$$

$$\underset{\sim}{s} = \frac{2\bar{P}_1' - \bar{P}_2' - \bar{P}_3'}{3r},$$

$$\underset{\sim}{a} = \underset{\sim}{n} \times \underset{\sim}{s},$$

$$\underset{\sim}{p} = \frac{\bar{P}_1' + \bar{P}_2' + \bar{P}_3'}{3}, \qquad (3.2)$$

and

$$| \bar{P}_1' - \bar{P}_2' |^2 = | \bar{P}_2' - \bar{P}_3' |^2 = | \bar{P}_3' - \bar{P}_1' |^2 = 3\, r^2 \qquad (3.3)$$

The only unknowns in the above equations are θ_{1i} values, which can be solved as follows.

3.1.2 SOLUTION OF θ_{1i} ANGLES

The method followed here is similar to the one presented in Nanua and Waldron [8].

Using (3.1)

$$\bar{P}_1' = \begin{bmatrix} L1 \cos \theta_{21} \cos \theta_{11} + R \cos \phi_1 \\ L1 \cos \theta_{21} \sin \theta_{11} + R \sin \phi_1 \\ L1 \sin \theta_{21} \end{bmatrix},$$

$$\bar{P}_2' = \begin{bmatrix} L2 \cos \theta_{22} \cos \theta_{12} + R \cos \phi_2 \\ L2 \cos \theta_{22} \sin \theta_{12} + R \sin \phi_2 \\ L2 \sin \theta_{22} \end{bmatrix} \quad \text{and}$$

$$\bar{P}_3' = \begin{bmatrix} L3 \cos \theta_{23} \cos \theta_{13} + R \cos \phi_3 \\ L3 \cos \theta_{23} \sin \theta_{13} + R \sin \phi_3 \\ L3 \sin \theta_{23} \end{bmatrix}.$$

Substituting above expressions in (3.3), we get the following three equations :

$$\cos \theta_{11} \left[A1 \cos \theta_{12} + C1\right] + \sin \theta_{11} \left[B1 \sin \theta_{12} + E1\right] + F1 \cos \theta_{12} + H1 \sin \theta_{12} + G1 = 0, \qquad (3.3.1)$$

$$\cos \theta_{12} \left[A2 \cos \theta_{13} + C2\right] + \sin \theta_{12} \left[B2 \sin \theta_{13} + E2\right] + F2 \cos \theta_{13} + H2 \sin \theta_{13} + G2 = 0 \text{ and} \qquad (3.3.2)$$

$$\cos \theta_{13} \left[A3 \cos \theta_{11} + C3\right] + \sin \theta_{13} \left[B3 \sin \theta_{11} + E3\right] + F3 \cos \theta_{11}$$

$+ H3 \sin \theta_{11} + G3 = 0.$ (3.3.3)

The coefficients like A1, A2 etc. appearing in (3.3.1) to (3.3.3) are listed in appendix I.

Equations (3.3.1), (3.3.2) and (3.3.3) are rewritten in a compact form as given below.

$$U1 \cos \theta_{11} + U2 \sin \theta_{11} + U3 = 0 \quad (3.4)$$

$$V1 \cos \theta_{12} + V2 \sin \theta_{12} + V3 = 0 \quad (3.5)$$

$$W1 \cos \theta_{11} + W2 \sin \theta_{11} + W3 = 0 \quad (3.6)$$

where

$U1 = A1 \cos \theta_{12} + C1,$

$U2 = B1 \sin \theta_{12} + E1,$

$U3 = F1 \cos \theta_{12} + H1 \sin \theta_{12} + G1,$

$V1 = A2 \cos \theta_{13} + C2,$

$V2 = B2 \sin \theta_{13} + E2,$

$V3 = F2 \cos \theta_{13} + H2 \sin \theta_{13} + G2,$

$W1 = A3 \cos \theta_{13} + F3,$

$W2 = B3 \sin \theta_{13} + H3,$

$W3 = C3 \cos \theta_{13} + E3 \sin \theta_{13} + G3.$

Solving (3.4) and (3.6) for $\sin \theta_{11}$ and $\cos \theta_{11}$ we get

$$\cos \theta_{11} = \frac{U2\ W3 - U3\ W2}{U1\ W2 - U2\ W1}$$

$$\sin \theta_{11} = \frac{U1\ W3 - U3\ W1}{U1\ W2 - U2\ W1} \quad (3.7)$$

Substituting the values of $\cos \theta_{11}$ and $\sin \theta_{11}$ from (3.7) in the identity

$$\cos^2 \theta_{11} + \sin^2 \theta_{11} - 1 = 0 \qquad (3.8)$$

we obtain

$$M1 \cos^2 \theta_{12} + M2 \sin^2 \theta_{12} + M3 \sin \theta_{12} \cos \theta_{12} + M4 \cos \theta_{12} + M5 \sin \theta_{12} + M6 = 0, \qquad (3.9)$$

where

$$M1 = F1^2 \left(W1^2 - W2^2 \right) + A1^2 \left(W3^2 - W2^2 \right) - 2\, A1\, F1\, W1\, W3.$$

$$M2 = B1^2 \left(W3^2 - W1^2 \right) + H1^2 \left(W1^2 - W2^2 \right) - 2\, B1\, H1\, W2\, W3,$$

$$M3 = 2\, F1\, H1 \left(W1^2 - W2^2 \right) - 2\, B1\, F1\, W2\, W3 - 2\, A1\, H1\, W1\, W3 + 2\, A1\, B1\, W1\, W2,$$

$$M4 = 2\, F1\, G1 \left(W1^2 - W2^2 \right) + 2\, A1\, C1 \left(W3^2 - W2^2 \right) - 2\, E1\, F1\, W2\, W3 + 2\, A1\, E1\, W1\, W2 - 2\, W1\, W3 \left(A1\, G1 + C1\, F1 \right),$$

$$M5 = 2\, B1\, E1 \left(W3^2 - W1^2 \right) + 2\, H1\, G1 \left(W1^2 - W2^2 \right) - 2\, C1\, H1\, W1\, W3 + 2\, B1\, C1\, W1\, W2 - 2\, W2\, W3 \left(B1\, G1 + E1\, H1 \right) \text{ and}$$

$$M6 = E1^2 \left(W3^2 - W1^2 \right) + C1^2 \left(W3^2 - W2^2 \right) + G1^2 \left(W1^2 - W2^2 \right) - 2\, E1\, G1\, W2\, W3 - 2\, C1\, K1\, W1\, W3 + 2\, C1\, E1\, W1\, W2.$$

From (3.5) one can write

$$\cos \theta_{12} = - \left(\frac{V3 + V2 \sin \theta_{12}}{V1} \right).$$

Substituting the above expression for $\cos \theta_{12}$ in (3.9), the equation simplifies to the following form :

where

$$N1 = M1\ V2^2 + M2\ V1^2 - M3\ V1\ V2,$$

$$N2 = 2\ M1\ V2\ V3 - M3\ V1\ V3 - M4\ V1\ V2 + M5\ V1^2 \text{ and}$$

$$N3 = M1\ V_3^2 - M4\ V1\ V3 + M6\ V1^2 .$$

Again using the identity,

$$\cos^2 \theta_{12} + \sin^2 \theta_{12} - 1 = 0 \qquad (3.11)$$

equation (3.5) can be rewritten in the form given below :

$$Q1 \sin^2 \theta_{12} + Q2 \sin \theta_{12} + Q3 = 0 \qquad (3.12)$$

where

$$Q1 = V2^2 - V1^2 ,$$

$$Q2 = 2\ V2\ V3 \quad \text{and}$$

$$Q3 = V3^2 - V1^2 .$$

Now, from equations (3.10) and (3.12) using Bezout's method to eliminate $\sin \theta_{12}$ we get

$$\begin{vmatrix} |N1\ Q2| & |N1\ Q3| \\ |N1\ Q3| & |N2\ Q3| \end{vmatrix} = 0,$$

where

$$|Ni\ Qj| = Ni\ Qj - Qi\ Nj.$$

i.e.,

$$\left[N1\ Q2 - N2\ Q1 \right] \left[N2\ Q3 - N3\ Q2 \right] - \left[N1\ Q3 - N3\ Q1 \right]^2 = 0 \qquad (3.13)$$

Equation (3.13) contains only sin θ_{13} and cos θ_{13}, which can be substituted by the tan half angle formulae, viz,

$$\sin\theta_{13} = \frac{2\tan\left(\frac{\theta_{13}}{2}\right)}{1+\tan^2\left(\frac{\theta_{13}}{2}\right)}$$

$$\cos\theta_{13} = \frac{1-\tan^2\left(\frac{\theta_{13}}{2}\right)}{1+\tan^2\left(\frac{\theta_{13}}{2}\right)}$$

Since Q1, Q2 and Q3 are fourth order polynomials in $\tan\left(\frac{\theta_{13}}{2}\right)$ and N1, N2 and N3 are eighth order polynomials in $\tan\left(\frac{\theta_{13}}{2}\right)$, the maximum order of $\tan\left(\frac{\theta_{13}}{2}\right)$ in (3.13) is 24. Once θ_{13} values are determined from (3.13), other two angles, viz, θ_{11} and θ_{12} follow from equations (3.5) and (3.6).

3.2 DIRECT KINEMATICS USING NUMERICAL METHOD

Solution of (3.3) by numerical techniques could be one of the methods of obtaining the platform matrix for a given set of six actuator lengths. However, if direct kinematics is needed as a feed back for known actuator lengths, measuring θ_{1i}'s using hardware in run time could be much more faster and convenient

than any of the numerical methods. A scheme similar to this has been implemented by Hirochika in [2].

In the present work, the inverse kinematic equations have been used to obtain direct solutions numerically. The technique used is Newton-Raphson method for systems of nonlinear algebraic equations. The development is presented in subsequent sections.

3.2.1 NEWTON-RAPHSON METHOD (FORMULATION)

Referring back to the inverse kinematics equations derived in the previous chapter, we have the following six equations :

$$Li = f_i(x, y, z, \alpha, \beta, \gamma)$$

$$Di = g_i(x, y, z, \alpha, \beta, \gamma)$$

$$i = 1, 2, 3. \qquad (3.14)$$

Equations (3.14) can be rewritten in the form given below.

$$\psi_j(x, y, z, \alpha, \beta, \gamma) = 0$$

$$j = 1,.....6 \qquad (3.15)$$

Let $(x_o, y_o, z_o, \alpha_o, \beta_o, \gamma_o)$ be an initial approximation for a zero of the system (3.15).

If $(x + h_x, y + h_y, z + h_z, \alpha + h_\alpha, \beta + h_\beta, \gamma + h_\gamma)$ is a zero of the system, then we have

$$\psi_j(x + h_x, y + h_y, z + h_z, \alpha + h_\alpha, \beta + h_\beta, \gamma + h_\gamma) = 0. \qquad (3.16)$$

Assuming that $\psi_j(\ )$ $j = 1,.....6$, are sufficiently differentiable, we expand (3.16) by Taylor's series to obtain

$$\psi_{j_o} + h_x \frac{\partial \psi_j}{\partial x_o} + h_y \frac{\partial \psi_j}{\partial y_o} + h_z \frac{\partial \psi_j}{\partial z_o} + h_\alpha \frac{\partial \psi_j}{\partial \alpha_o} + h_\beta \frac{\partial \psi_j}{\partial \beta_o} + h_\gamma \frac{\partial \psi_j}{\partial \gamma_o} +$$

higher order terms..... = 0

$j = 1, ...6,$

(3.17)

where

$$\psi_{j_o} = \psi_j(x_o, y_o, z_o, \alpha_o, \beta_o, \gamma_o),$$

$$\frac{\partial \psi_j}{\partial x_o} = \left(\frac{\partial \psi_j}{\partial x} \right)_{x = 0} \quad \text{etc.}$$

Neglecting the second and higher order terms, we obtain the system of linear equations :

$$h_x \frac{\partial \psi_1}{\partial x_o} + h_y \frac{\partial \psi_1}{\partial y_o} + h_z \frac{\partial \psi_1}{\partial z_o} + h_\alpha \frac{\partial \psi_1}{\partial \alpha_o} + h_\beta \frac{\partial \psi_1}{\partial \beta_o} + h_\gamma \frac{\partial \psi_1}{\partial \gamma_o} = - \psi_{1_o}$$

$$h_x \frac{\partial \psi_2}{\partial x_o} + h_y \frac{\partial \psi_2}{\partial y_o} + h_z \frac{\partial \psi_2}{\partial z_o} + h_\alpha \frac{\partial \psi_2}{\partial \alpha_o} + h_\beta \frac{\partial \psi_2}{\partial \beta_o} + h_\gamma \frac{\partial \psi_2}{\partial \gamma_o} = - \psi_{2_o}$$

$$h_x \frac{\partial \psi_3}{\partial x_o} + h_y \frac{\partial \psi_3}{\partial y_o} + h_z \frac{\partial \psi_3}{\partial z_o} + h_\alpha \frac{\partial \psi_3}{\partial \alpha_o} + h_\beta \frac{\partial \psi_3}{\partial \beta_o} + h_\gamma \frac{\partial \psi_3}{\partial \gamma_o} = - \psi_{3_o}$$

$$h_x \frac{\partial \psi_4}{\partial x_o} + h_y \frac{\partial \psi_4}{\partial y_o} + h_z \frac{\partial \psi_4}{\partial z_o} + h_\alpha \frac{\partial \psi_4}{\partial \alpha_o} + h_\beta \frac{\partial \psi_4}{\partial \beta_o} + h_\gamma \frac{\partial \psi_4}{\partial \gamma_o} = - \psi_{4_o}$$

$$h_x \frac{\partial \psi_5}{\partial x_o} + h_y \frac{\partial \psi_5}{\partial y_o} + h_z \frac{\partial \psi_5}{\partial z_o} + h_\alpha \frac{\partial \psi_5}{\partial \alpha_o} + h_\beta \frac{\partial \psi_5}{\partial \beta_o} + h_\gamma \frac{\partial \psi_5}{\partial \gamma_o} = - \psi_{5_o}$$

$$h_x \frac{\partial \psi_6}{\partial x_o} + h_y \frac{\partial \psi_6}{\partial y_o} + h_z \frac{\partial \psi_6}{\partial z_o} + h_\alpha \frac{\partial \psi_6}{\partial \alpha_o} + h_\beta \frac{\partial \psi_6}{\partial \beta_o} + h_\gamma \frac{\partial \psi_6}{\partial \gamma_o} = - \psi_{6_o}$$

(3.18)

which can readily be solved for h_x, h_y, h_z, h_α, h_β and h_γ. Here, Cramer's rule has been employed to solve the above linear equations and to obtain a new approximation given by,

$$x_1 = x_o + \frac{|J_1|}{|J|}$$

$$y_1 = y_o + \frac{|J_2|}{|J|}$$

$$z_1 = z_o + \frac{|J_3|}{|J|}$$

$$\alpha_1 = \alpha_o + \frac{|J_4|}{|J|}$$

$$\beta_1 = \beta_0 + \frac{|J_5|}{|J|}$$

$$\gamma_1 = \gamma_0 + \frac{|J_6|}{|J|}$$

assuming $|J| \neq 0$ (3.19)

where

J is a [6 X 6] matrix containing the coefficients of h_x, h_y, h_z, h_α, h_β and h_γ in equations (3.18), which are nothing but the partial derivatives of $\psi_j(\ )$ with respect to six variables and the matrix is generally referred to as a *Jacobian* [see article 3.3] as it fundamentally relates the rates of leg motions to those of platform motions,

J_j is the matrix J, with its j^{th}column replaced by a [6 X 1] column vector consisting of the values on the right side of equation (3.18) and

$|J|, |J_j|$ respectively, represent the determinant of the matrices J and J_j.

3.2.2 INITIAL SOLUTION AND CONVERGENCE

The method discussed above needs a rough estimate of inital solutions, which has been given under following approximations :

(i) xo, yo and zo assuming $\alpha = 0$, $\beta = 0$ and $\gamma = 0$,

(ii) approximate α_o and β_o values using z coordinate of each corner of platform,

(iii) $\gamma_o = 0$.

The general algorithm works as follows :

(i) find inital solutions as discussed above,

(ii) find x_1, y_1..etc. using (3.19),

Fig.3.2 Initial & actual solution(Li=lmean,D1=D2=dmean)

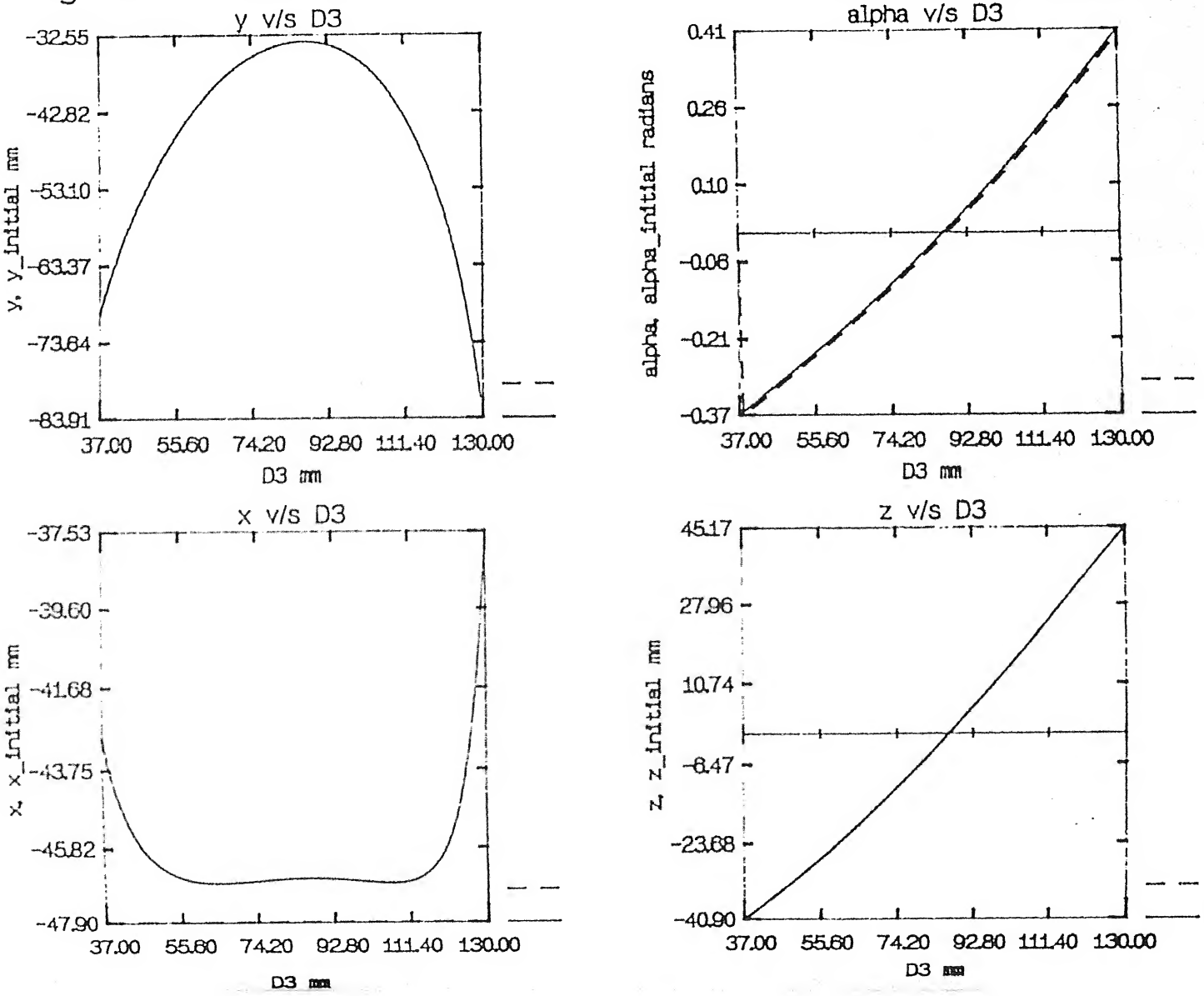

Fig. 3.2 (contd)

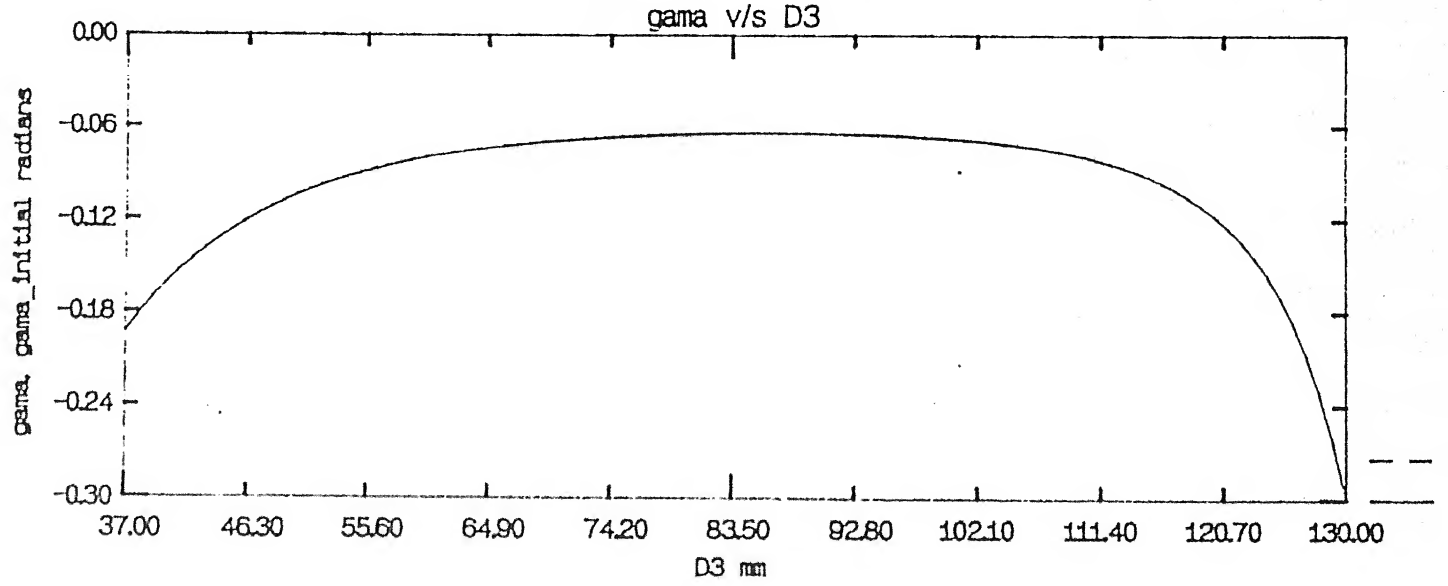
gama v/s D3
gama, gama_initial radians
0.00
-0.06
-0.12
-0.18
-0.24
-0.30
37.00
46.30
55.60
64.90
74.20
83.50
92.80
102.10
111.40
120.70
130.00
D3 mm

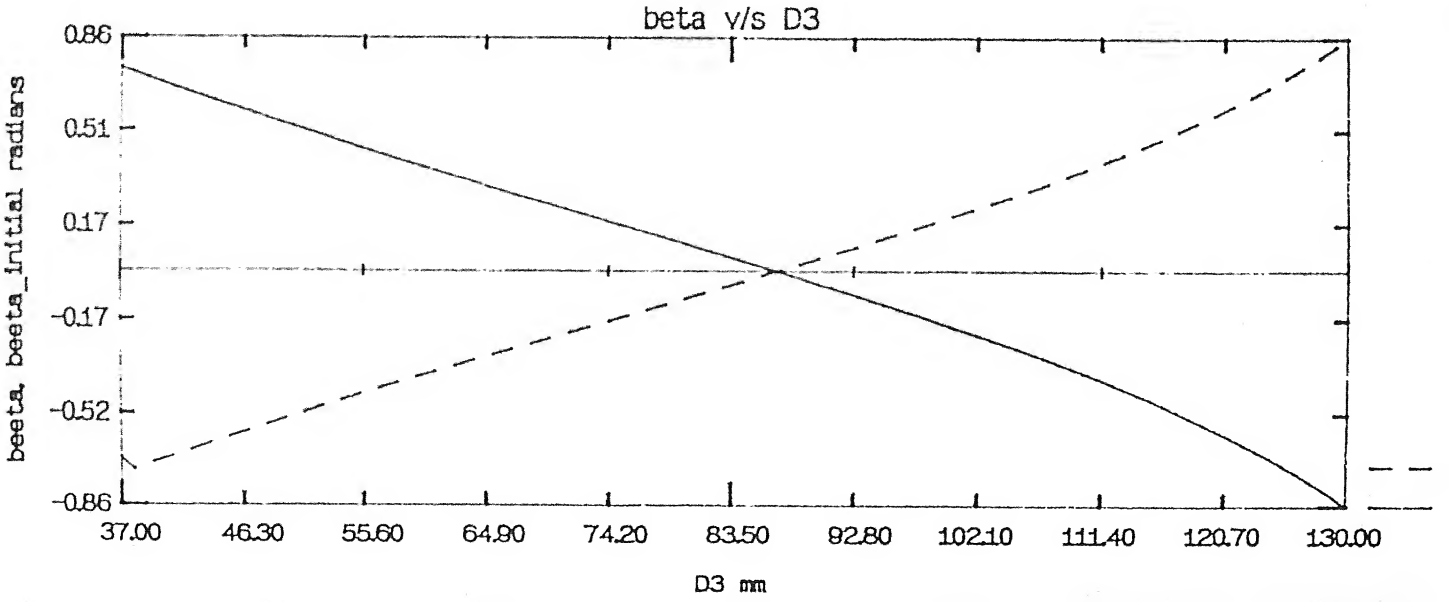
beta v/s D3
beeta, beeta_initial radians
0.86
0.51
0.17
-0.17
-0.52
-0.86
37.00
46.30
55.60
64.90
74.20
83.50
92.80
102.10
111.40
120.70
130.00
D3 mm

(iii) compute $\psi_j(\ )$ value using (3.15) and check if

abs(ψ_j) $\leq$ 0.001, for j = 1, ...6.

which signals the convergence being attained.

Else repeat (ii).

The plots depicting the relationship between the initial and the actual solutions have been shown in Fig. 3.2. The convergence of solutions is usually within five iterations which can be seen in the table below. It is to be noted here that for these computations, the coordinate and the angle conventions used are slightly different from the one mentioned while deriving control equations. Also, h_{usb} has been assumed zero for simplicity.

Table showing the convergence of the Newton-Raphson algorithm used for solving direct position kinematics

(all lengths are in mm and angles are in degrees)

L1 = 178.0, L2 = 148.0, L3 = 243.0,

D1 = 147.0 D2 = 156.0, D3 = 202.0.

	x	y	z	α	β	γ
	Initial solution					
	-14.80219	54.21995	00.00000	34.19910	-06.04896	00.00000
1	-36.33405	63.46407	-05.66178	30.71583	-39.17723	-07.02912
2	-29.10054	48.91883	-05.66178	30.78249	-41.20569	-09.19877
3	-28.58534	48.59558	-05.66178	30.78251	-41.23778	-09.90913
4	-28.58330	48.59109	-05.66178	30.78251	-41.23779	-09.91303

Figure 3.2 also shows the effect of the lower actuator displacements on the position and orientation of the platform.

3.3 SINGULAR CONFIGURATION

The *jacobian* of a manipulator is generally defined as the matrix representing the transformation mapping the joint rate into the cartesian velocities. However, in the case of parallel manipulators the complexity of the direct and inverse kinematic problems are exchanged. The *jacobian* matrix for an SPM can be defined using the inverse kinematic equations as given below.

$$J\,\dot{c} = \dot{l} \qquad (3.20)$$

where

$\dot{c} = [\ \dot{x},\ \dot{y},\ \dot{z},\ \dot{\alpha},\ \dot{\beta},\ \dot{\gamma}\ ]^T$ is the vector of cartesian velocities and

$\dot{l} = [\ \dot{L1},\ \dot{L2},\ \dot{L3},\ \dot{D1},\ \dot{D2},\ \dot{D3}\ ]^T$ is the vector of actuator speed.

Using (3.14), a J matrix can be defined similar to the one described before.

$$J = \begin{bmatrix} \frac{\partial L1}{\partial x} & \frac{\partial L1}{\partial y} & \frac{\partial L1}{\partial z} & \frac{\partial L1}{\partial \alpha} & \frac{\partial L1}{\partial \beta} & \frac{\partial L1}{\partial \gamma} \\ \frac{\partial L2}{\partial x} & \frac{\partial L2}{\partial y} & \frac{\partial L2}{\partial z} & \frac{\partial L2}{\partial \alpha} & \frac{\partial L2}{\partial \beta} & \frac{\partial L2}{\partial \gamma} \\ \frac{\partial L3}{\partial x} & \frac{\partial L3}{\partial y} & \frac{\partial L3}{\partial z} & \frac{\partial L3}{\partial \alpha} & \frac{\partial L3}{\partial \beta} & \frac{\partial L3}{\partial \gamma} \\ \frac{\partial D1}{\partial x} & \frac{\partial D1}{\partial y} & \frac{\partial D1}{\partial z} & \frac{\partial D1}{\partial \alpha} & \frac{\partial D1}{\partial \beta} & \frac{\partial D1}{\partial \gamma} \\ \frac{\partial D2}{\partial x} & \frac{\partial D2}{\partial y} & \frac{\partial D2}{\partial z} & \frac{\partial D2}{\partial \alpha} & \frac{\partial D2}{\partial \beta} & \frac{\partial D2}{\partial \gamma} \\ \frac{\partial D3}{\partial x} & \frac{\partial D3}{\partial y} & \frac{\partial D3}{\partial z} & \frac{\partial D3}{\partial \alpha} & \frac{\partial D3}{\partial \beta} & \frac{\partial D3}{\partial \gamma} \end{bmatrix} \qquad (3.21)$$

The manipulator *jacobian* J is configuration dependent. For serial manipulators, the J matrix and its singularities have been studied extensively and can be geometrically interpreted. For the parallel manipulators, such studies have not been carried out.

This can be an area of future study.

An SPM can be assembled in many modes, similar to the classical elbow-up and elbow-down solutions of a four-bar linkages. Different assembly modes, for identical leg lengths can give rise to varying platform positions. At the points of singularity, the platform position can be simultaneously attained by two assembly modes, and they represent the points where assembly modes can be switched. At these points, the manipulator gains an additional degree-of-freedom or compliance, which is undesireable from a control standpoint. One of the difficulties can be explained as follows: The mean position defined [see section 2.4.1] is one of the possible assembly configurations keeping all the actuators at their respective mean lengths (l_{mean} and d_{mean}). Suppose, the platform moves to a new position and orientation which is singular or near singular. At such a position, the manipulator gains unwanted degree-of-compliance and may switch assembly modes. Now, if all the actuators are moved back to the initial mean length (l_{mean} and d_{mean}), the manipulator may not be brought back to the chosen initial assembly configuration.

During any controlled sequence of end effector guidance in an SPM, it is essential to preserve configuration continuity, within what can be termed assembly mode continuity [7]. This is generally be done by defining an optimality index (called condition number) as a function of manipulator *jacobian* [5]. This index which can be thought of a measure of the distance to singularity are maximized along a partially defined trajectory (i.e., a trajectory defined with say, only five variables, so that the sixth variable can be quantified using singularity

minimization criterion). This implementation for three degrees-of-freedom planar and spherical manipulators has been considered by Gosselin and Angles in [5].

3.4 SIMULATION OF MANIPULATOR GEOMETRY

A simple geometric simulation of an SPM has been carried out with the following objectives :

(i) As a starting point in visualizing the manipulator and its movements.

(ii) As a predesign aid in verifying various link parameters.

(ii) As a six dimensional representation of the results of direct position kinematics.

The aid used here is *starbase* graphic software. Few such results have been illustrated in Figs. 3.3 and 3.4.

Figure 3.3(a) shows complete planar movements of the platform at Z = 0 plane. This has been obtained keeping any two of the three ULA's at Lmin and varying the remaining one from Lmin to Lmax. Figure 3.3(b) is similar to Fig. 3.3(a), except two of the three ULA's have been kept at Lmax. These 2D representations give an approximate idea of the sweep area of the platform at Z = 0 plane.

Figure 3.4 illustrates various positions and orientations of the platform by varying an LLA, keeping remaining two LLA's at D_{mean} and all ULA's at Lmax. In the present design, this movement does have actuator interference as well as vanishing work space if two LLA's are kept near Dmin or Dmax.

Fig.3.3(a) Planar movements of SPM

(Two of the three ULA's at Lmax)

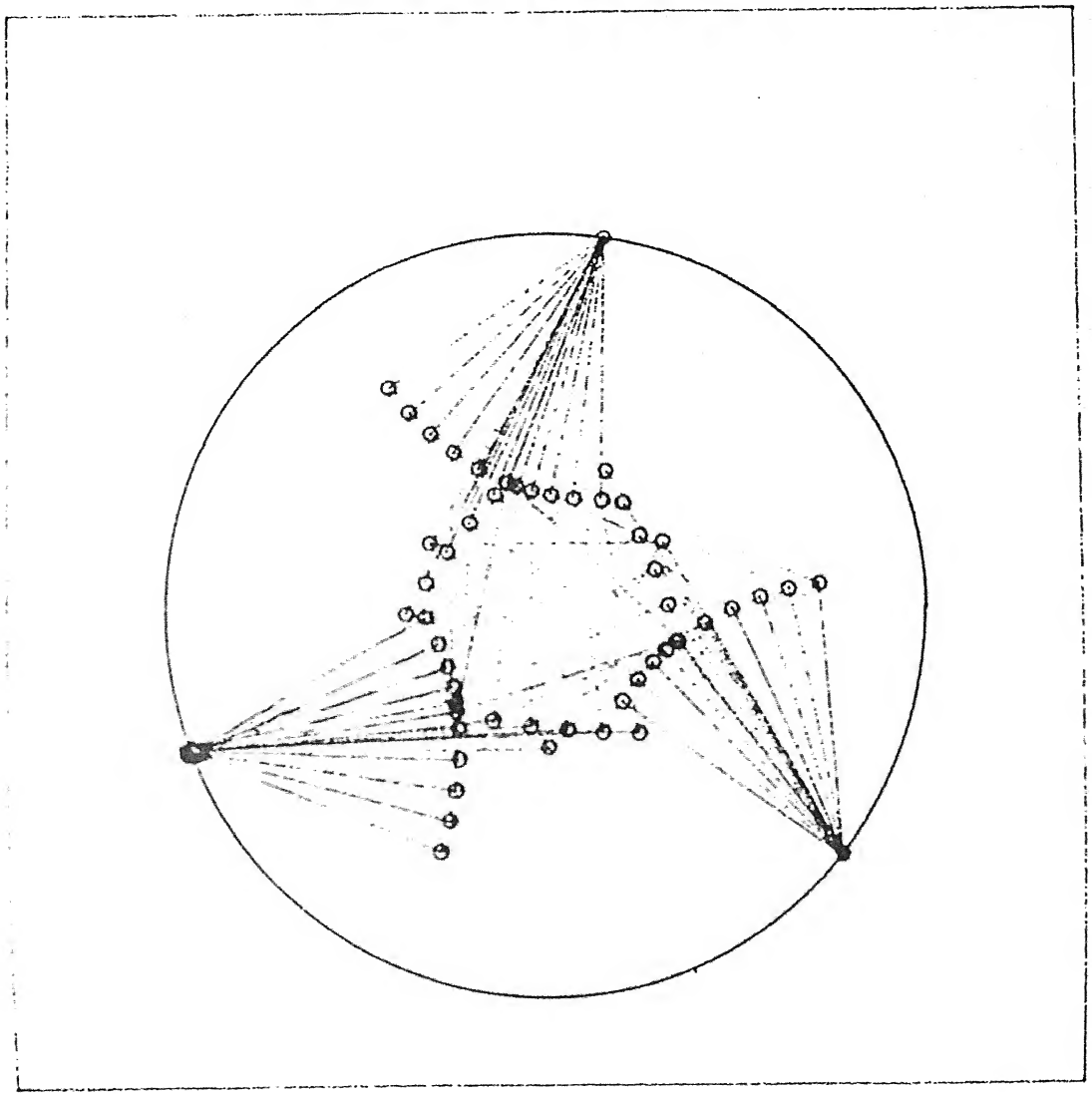

Fig.3.3(b) Planar movements of SPM

(Two of the three ULA's at Lmin)

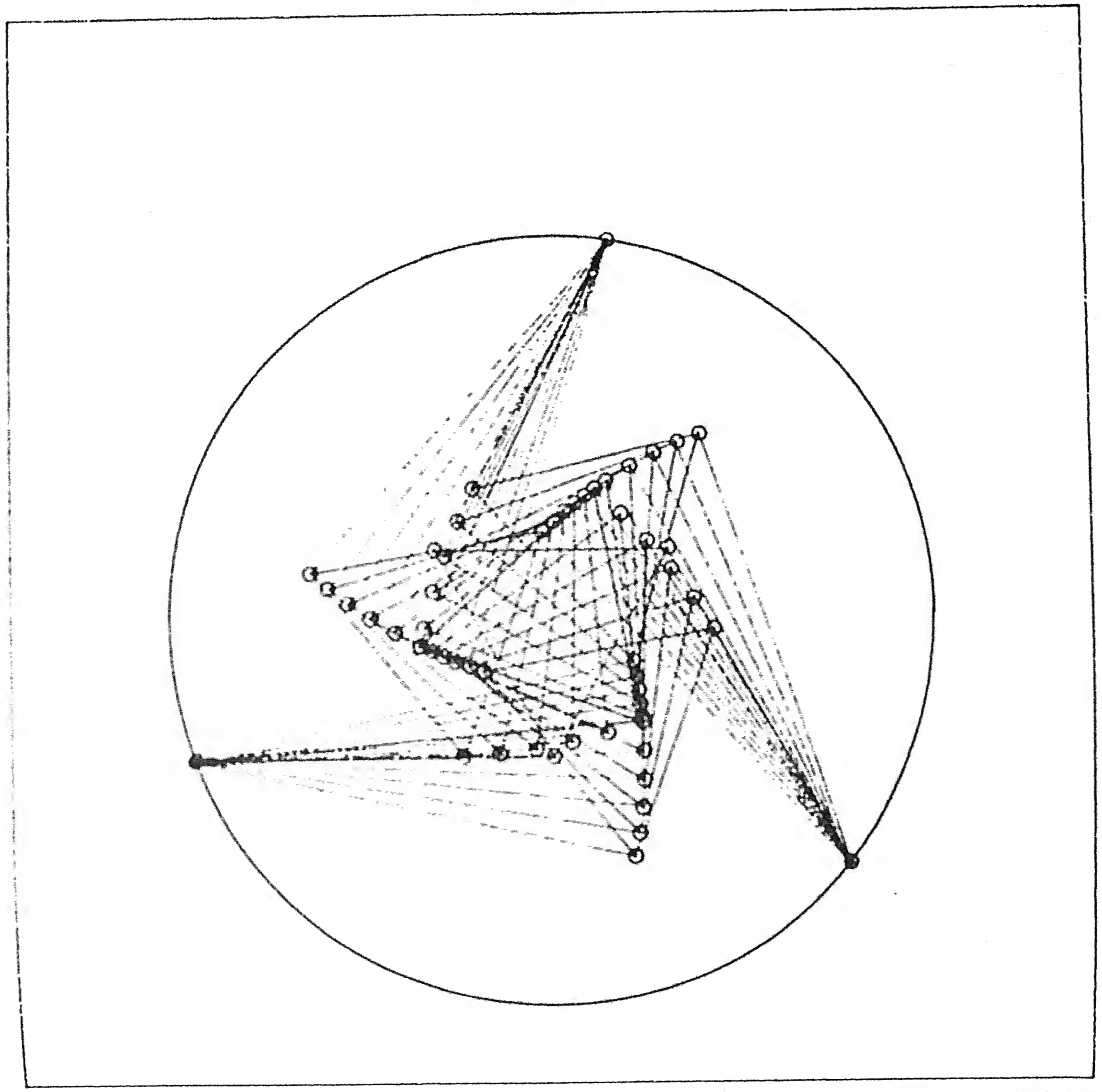

Fig.3.4 3D simulation of SPM movements

3.5 DISCUSSIONS

In a series actuated manipulators, the problem of direct kinematics is easier, yields only one end effector configuration and hence, is a convenient means for mechanism synthesis. For a parallel manipulator like SPM, the solutionof the direct position kinematics problem in closed form is complex. Closed form approach, hence has not been used, instead, a numerical method has been employed for simulating manipulator movements.

There are special configurations where the manipulator gains a degree-of-compliance. To ensure that the manipulator avoids any special configurations, proper trajectory planning is needed. The manipulator's proximity to an uncertain configuration due to singularity or near singularity, can be verified only by tracking θ_{1i} angles. An analytical direct position kinematics solution indicates possible position and orientations of the platform for known set of actuator lengths. It does not explicitly indicate which the particular position and orientation have been attained.

CHAPTER 4

KINEMATIC DESIGN OF STEWART PLATFORM MANIPULATOR

The present work, which aims at developing a Stewart Platform Manipulator is not an analytic design with specified performance criteria, rather an experiemental approach to develop a device for future research and evaluation. In addition, the manipulator is not targeted to be used for a specific task. This made the design more difficult as there were no constraints other than the idea of the Stewart platform.

The design aim was to build an original Stewart Platform Manipulator [Fig. 1.4]. We decided to use a motor lead-screw combination as the linear actuator as we had know how to control them. One of the targets was to achieve a large work volume relative to the floor space the device occupied.

4.1 CHOOSING TRANSMISSION RATIO - A BALL SCREW MODEL

The choice of actuators and transmissions has a significant effect on the time required to perform a specific machine task. For a system operating with mechanical constraints such as bounds on motor speed, designing for greatest achievable acceleration does not always minimize travel time [12].

An actuator with one degree-of-freedom has been shown in Fig. 4.1(a).

Let

M be the sliding mass in the screw pair,

J the rotary inertia of the motor (torque source),

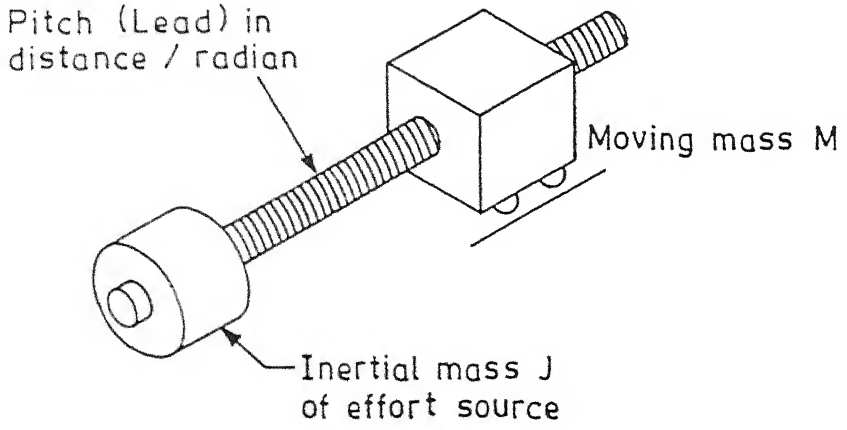

Fig. 4.1(a). A servo model.

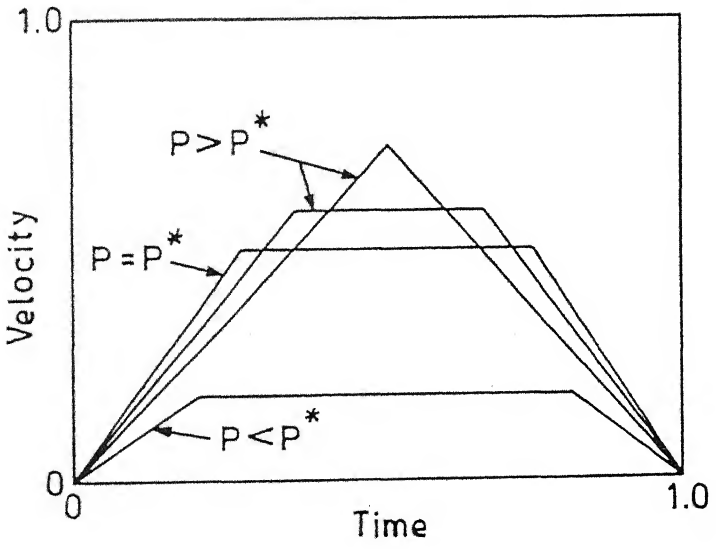

Fig. 4.1(b). Typical incremental move velocity profiles.

τ the torque produced and

P transmission ratio(distance/radian). This is the lead (or pitch in a single start thread) and is equal to the ratio of output translational velocity to input angular velocity.

Then the equation of motion for the system shown in Fig. 4.1(a) is

$$\tau = \left(\frac{J}{P} + M P\right) \alpha \qquad (4.1)$$

where α is the output acceleration. For an available maximum value of source torque (τ), minimizing the term within the bracket will yield maximum α value. Hence, a value of P can be found which minimizes the quantity in bracket, as given below :

$$\frac{\partial}{\partial P}\left(\frac{J}{P} + M P\right) = 0$$

$$P^{*} = \sqrt{\frac{J}{M}} \qquad (4.2)$$

where P^{*} is the transmission ratio that produces the greatest system acceleration for a given actuator torque.

Fig. 4.1(b) shows the velocity profile for a DC servo motor (with top speed limited to ω_{max}) for different P values. For the case in which the system does not have a limiting peak velocity, the transmission ratio that minimizes the total move time is $P = P^{*}$.

However, the transmission ratio that minimizes the time required to move through a specified travel d where the motor has a maximum angular velocity $\omega = \omega_{max}$, is given by

$$P_{opt} = \sqrt[3]{\frac{\tau\, d}{2\, M\, \omega_{max}^2}} \quad . \qquad (4.3)$$

The transmission ratio of choice for a given system design is that which does the best job of minimizing move time throughout the range of intrest of moves [12].

In the present case, we have assumed the following parameters for the actuators :

Maximum torque of DC servo motor (τ_{max}) = 25 X 10^{-2} N m,

Motor inertia (J) = 0.1 X $\left[0.04\right]^2$ N m^2,

Peak angular speed at the coupling (ω_{max}) = 2π radian/second,

Pitch of the lead-screw (P) = $\frac{1.75}{2\pi}$ X 10^{-3} m/radian and

Sliding mass (M) = 0.5 Kg.

Total time required for a ULA to execute full stroke (2δ) can be computed using

Total time = time to reach the peak velocity (t_p) +

time of travel with the peak velocity (t_s).

(4.4.1)

The time required to reach peak velocity ($P\omega_{max}$) is given by

$$t_p = \frac{\omega_{max}\left[J + M\, P^2\right]}{\tau} \qquad (4.4.2)$$

which is negligibly small. The time required to travel 2δ distance is

$$t_s = \frac{2\delta}{P\, \omega_{max}}, \qquad (4.4.3)$$

which is approximately 60 secs.

The lead-screw we used is M12 X 1.75 (single start) which can give a control resolution of $\frac{1.75}{180}$ mm, where 180 is the number of pulses per revolution that the encoder can generate. Use of multistart thread or high pitch has practical limitation as far

as fabrication is concerned. also this reduces the control resolution.

4.2 GENERAL MOTION ANALYSIS AND MANIPULATOR RANGE

Referring to the inverse position kinematic equations, it can be stated that the actuator lengths are functions only of the positions of corners of the platform. The corner positions in turn determine the orientation of the platform plane. There is no single link which is associated with a particular degree-of-freedom of the platform.

Given an SPM in the mean position,

- Varying the lengths of the ULA independently gives x, y and γ movements to the platform,
- Varying ULA's simultaneously by equal amount gives rotational (γ) movement about an axis normal to the plane of platform and inclination of that axis to Z_v is decided by the lengths of LLA's,
- Varying a LLA independently or simultaneously results in positional as well as angular movements of the platform.

Referring back to Fig. 2.3, ULA 1 is parallel to X_v axis, ULA 2 and ULA 3 are inclined at 60^o and -60^o respectively with the X_v axis at the mean position. Keeping the combined rotation matrix (orientation matrix) as an identity (I), the inverse kinematic equations (2.7) and (2.11) will simplify to the following form :

$$L1^2 = l_{mean}^2 + 2\, l_{mean}\, x_p + x_p^2 + y_p^2 + z_p^2$$

$$L2^2 = l_{mean}^2 - l_{mean}\, x_p - \sqrt{3}\; l_{mean}\, y_p + x_p^2 + y_p^2 + z_p^2$$

$$L3^2 = l_{mean}^2 - l_{mean}\, x_p + \sqrt{3}\; l_{mean}\, y_p + x_p^2 + y_p^2 + z_p^2 \qquad (4.5.1)$$

$$D1^2 = K_1 + K_2\left[\frac{z_p}{L1}\right]$$

$$D2^2 = K_1 + K_2\left[\frac{z_p}{L2}\right]$$

$$D3^2 = K_1 + K_2\left[\frac{z_p}{L3}\right] \qquad (4.5.2)$$

h_{usb} has not been considered in these analysis. Non inclusion of h_{usb} will not cause any significant alteration in the manipulator workspace, manipulator occupied space etc.

Maximum movement of the platform in X_v direction when $y_p = 0$, $z_p = 0$ and $[\underset{\sim}{n}, \underset{\sim}{s}, \underset{\sim}{a}] = I$, can be obtained using (4.5.1) and is given by

$$x_{max} = \delta \;,\; x_{min} = -\delta \quad \text{or}$$

$$x_{range} = 2\,\delta \;, \qquad (4.6.1)$$

which is limited by the stroke length of ULA 1. This range is guaranteed only when there is no movement in all other directions.

Maximum movement in the Y_v direction is obviously larger than that in the X_v direction since the stroke of ULA 2 and ULA 3 are fully utilized, also ULA 1 does not impose any constraint.

$$y_{max} = \frac{y_{range}}{2} \;,$$

$$y_{min} = -\,y_{max} \;,$$

where y_{range}, using (4.5.1), is given by

$$y_{range} = 2\left(\frac{2\delta}{\sqrt{3}}\right) \qquad (4.6.2)$$

This range is for the situation when all movements except in x and y directions are constrained. Thus, x_{range} and y_{range} are only dependent on the stroke length of the actuators.

Consider the equation for the length of LLA,

$D_i^2 = K_1 + K_2 \sin\theta_{2i}$ which can be rewritten as follows :

$$\sin\left(\theta_{2i\,max}\right) = \frac{D_{i\,max}^2 - K_1}{K_2},$$

$$\sin\left(\theta_{2i\,min}\right) = \frac{D_{i\,min}^2 - K_1}{K_2},$$

$$dmean = \sqrt{K_1} \quad \text{and}$$

$$\left(\theta_{2i}\right)_{range} = \sin^{-1}\left[\frac{D_{i\,max}^2 - dmean^2}{K_2}\right] - \sin^{-1}\left[\frac{D_{i\,min}^2 - dmean^2}{K_2}\right]. \qquad (4.6.3)$$

D_{max} and D_{min} being limited by the stroke of the actuator, reducing K_2 increases the swing angle of ULA about the horizontal axis of the RR-joint. In the present design h_spp has been chosen to ensure proper clearance between the lower actuator and the upper support ring.

Consider the displacement of a corner of the platform in Z_v direction.

for $x_p = 0$, $y_p = 0$ and $[\underset{\sim}{n}, \underset{\sim}{s}, \underset{\sim}{a}] = I$

$$z_{max} = l_{mean} \tan\left(\theta_{2i\,max}\right),$$

$$z_{min} = l_{mean} \tan\left(\theta_{2i\,min}\right).$$

$$z_{range} = z_{max} - z_{min}. \qquad (4.6.4)$$

For a designed θ_{2i} range, increasing the ULA mean length increases z_{range}. This increases the support ring radius R for a given size r of the platform [see section 4.4.4].

From the inverse kinematic equations developed in the section 2.4.2, if $x_p = 0$, $y_p = 0$, $z_p = 0$

$$L1^2 = l_{mean} + 2\, l_{mean}\, fx_1 + fx_1^2 + fy_1^2 + fz_1^2$$

$$L2^2 = l_{mean} - l_{mean}\, fx_2 - \sqrt{3}\, l_{mean}\, fy_2 + fx_2^2 + fy_2^2 + fz_2^2$$

$$L3^2 = l_{mean} - l_{mean}\, fx_3 + \sqrt{3}\, l_{mean}\, fy_3 + fx_3^2 + fy_3^2 + fz_3^2$$

(4.7.1)

$$D1^2 = K_1 + K_2\, \frac{fz_1}{L1}$$

$$D2^2 = K_1 + K_2\, \frac{fz_2}{L2}$$

$$D3^2 = K_1 + K_2\, \frac{fz_3}{L3} \qquad (4.7.2)$$

where $[\, fx_i,\ fy_i,\ fz_i \,]^T$ is the displacement of i^{th} corner in x_v, y_v, z_v directions due to the rotation of the platform about the axes of fixed reference coordinate system. These corner displacements are functions of r, the platform circle radius. Smaller the value of r, larger will be the orientability of the platform. This also increases the number of modes of actuator interference.

Selection of the present scheme automatically gives large

z-movements of each leg assembly. The x and y movements are smaller. Consequently, the platform has large z-movement, large α and β movements are obtained by changing the z positions of the points of attachment with respect to each other. However the x and y movements of the platform are limited and so is the γ-movement. The amount of γ-movement could well be the ideal basis for deciding the platform radius (r).

4.3 INTERFERENCE AND JOINT LIMITATIONS

Two other important considerations during the design of an SPM are

(i) Link interferences and

(ii) Limitation on the rotation of spherical joints.

4.3.1 LINK INTERFERENCES

For link interference studies, only the support structure and ULA are important since the LLA will not usually interfere with any other link.

Referring to Fig.4.2, a tripod support structure, whose corners support RR-joints will interfere with leg movements (case ii). On the other hand a tripod support structure midpoints of whose sides are used as support points [case (i)], will reduce the compactness [see section 4.5] of SPM by about 50 %. In the latter case, the maximum bending movement at the tripod side is approximately 3-4 times that in the former case. This can be taken care of by necessary modification in the cross section of the support frames. Another problem with triangular support

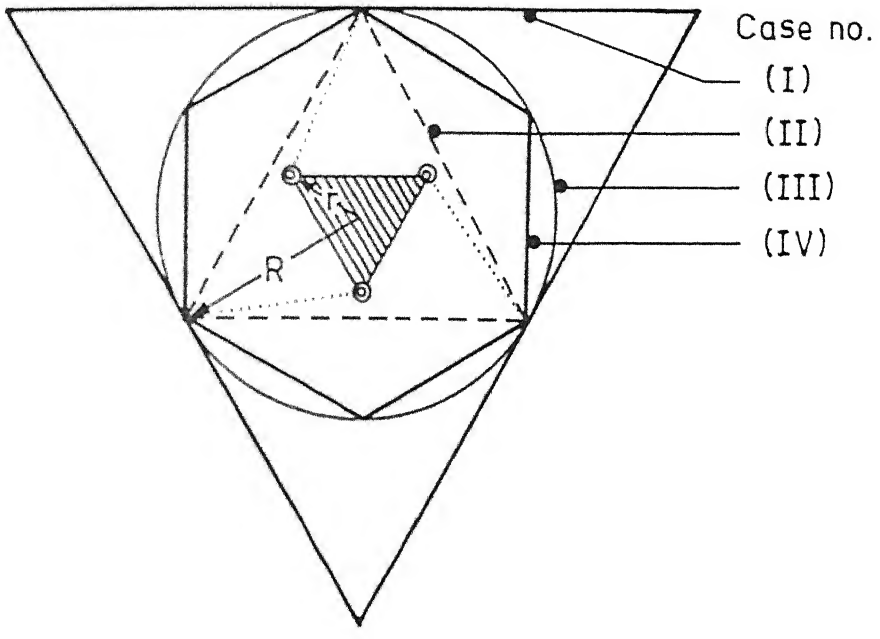

Fig. 4.2. Possible support structure designs.

structures is that it spoils the aesthetic look of an SPM setup, which is something that we thought, should not be neglected in the design. The present design uses a circular support frame [case (iii)] which we have referred to as support ring in chapter 2. We have not considered any other shape of support frame e.g., hexagonal, as they make the fabrication complicated.

The twist, γ-movement of the platform at x = 0, y = 0, z = 0 plane can have a maximum value of $\pm \frac{\pi}{3}$ provided the side of the platform triangle is equal to or less than the stroke length of an ULA. This causes the ULA to interfere with each other at the end of stroke and induces instability at the start of the stroke. This situation has been circumvented in the present design. If $\left[Li\right]_{max} \geq$ support distance (support distance is equal to $\sqrt{3}R$), full stroke of ULA can not be realized at least in x = 0, y = 0, z = 0 plane. Hence proper care in choosing $\left[\frac{\delta}{l_{mean}}\right]$ or $\left[\frac{\delta}{r}\right]$ ratio is necessary to realize full stroke of any ULA, when the other two ULA's are in any arbitrary position.

If $\alpha = 0$, $\beta = 0$, using (4.7.1) we get

$$Li^2 = l_{mean}^2 + \sqrt{3}\, l_{mean}\, r + r^2 \quad \text{for } \gamma = \frac{\pi}{3} \text{ and} \qquad (4.8.1)$$

$$Li^2 = l_{mean}^2 - \sqrt{3}\, l_{mean}\, r + r^2 \quad \text{for } \gamma = -\frac{\pi}{3}. \qquad (4.8.2)$$

Suppose $Li < \left[l_{mean} + \delta\right]$ and

$Li > \left[l_{mean} - \delta\right]$

respectively, produces $\frac{\pi}{3}$ and $-\frac{\pi}{3}$ rotations about reference Z-axis (Z_v). With such designs [see Fig. 4.3], the full stroke of ULA's is not possible.

Instability occurs if the centroid of the platform support points and two ends of any one leg fall in line [1]. A simulation, where each ULA is along the line joining its RR-joint

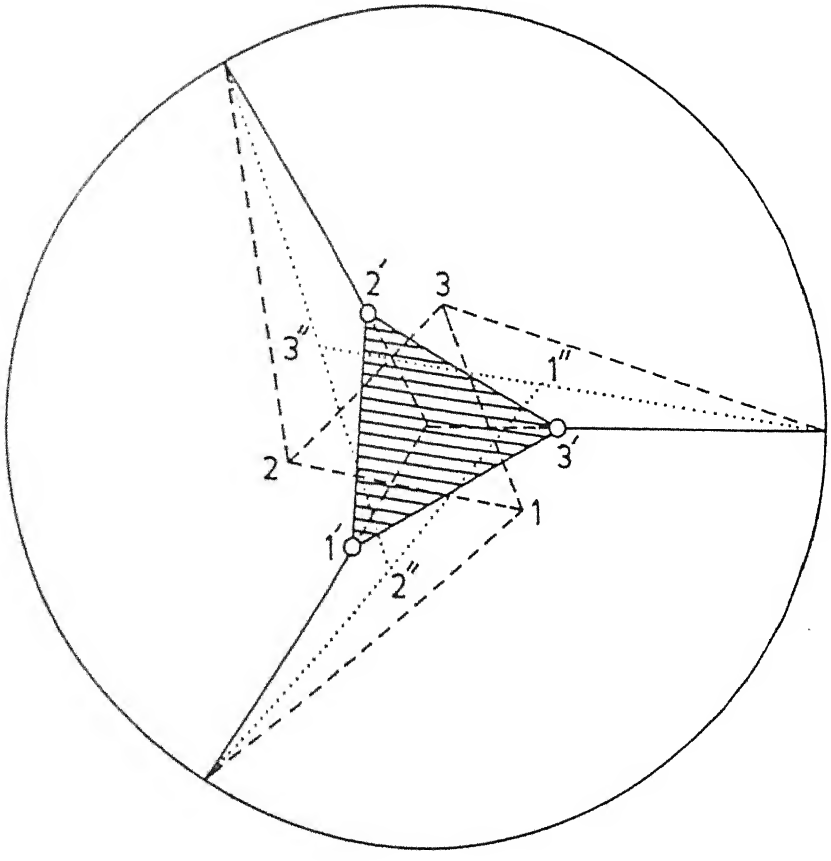

Fig. 4.3. Simulation of a platform with $\pm \pi/3$ rotation about Z_w.

1 2 3 : Mean position
1' 2' 3' : $-\pi/3$ rotation (Unstable position)
1" 2" 3" : $+\pi/3$ rotation (Interference)

to the centroid of the platform is shown in Fig. 4.3. Such a situation may give rise to the following situations:

* Length of ULA can not be decreased beyond its present length.
* It is difficult to maintain initial assembly mode continuity when the platform is moved to next desired position.

A design where $\left(l_{mean} - \delta + r \right)^2 > R^2$

or $$l_{mean} > \frac{\delta^2 - 2 r \delta}{2 \delta - 2 r} \qquad (4.9)$$

can prevent the manipulator from reaching such a configuration at $z = 0$ plane. This is not a practical realization problem as the manipulator can be made to avoid such a configuration.

The present design is interference free at $x = 0, y = 0, z = 0$ plane, but actuators may interfere at extreme z values (or at extreme α, β values). This is because the spherical joints and ULA do not have a common axis at the mean position. Lastly, designing for interference (limiting actuator movements) at $x = 0$ $y = 0$, $z = 0$ plane at the cost of getting good angular movements in other planes could also be the better consideration in deciding the platform size.

4.3.2 LIMITATION OF SPHERICAL JOINTS

A ball-and-socket joint [Fig. 4.4(a)] should ideally rotate freely with respect to all three cartesian axes. In practice, however, this is not achievable. This motion of actual ball joints is always restricted because of its physical dimensions. A ball joint includes three parts, the ball head, socket and the

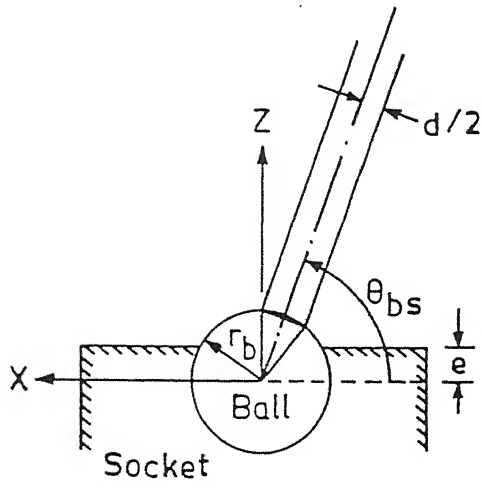

Fig. 4.4(a). A ball and socket joint.

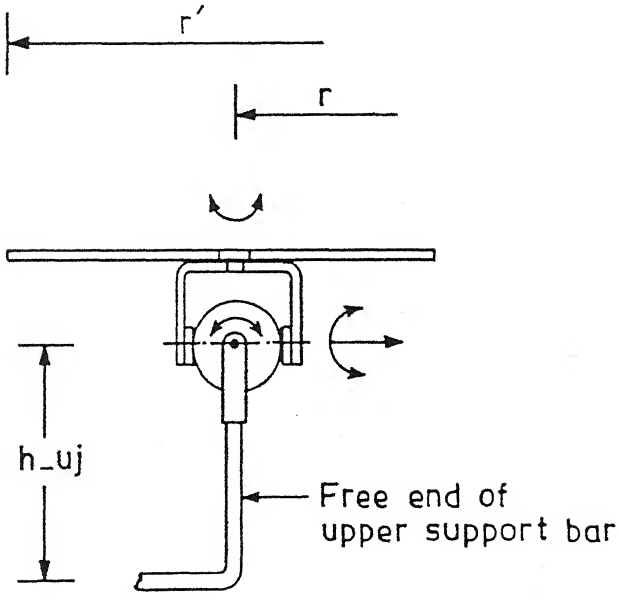

Fig. 4.4(b). A three-axis joint (Universal type)

connecting leg. Referring to Fig. 4.4(a), let

r_b = radius of ball head,

$\frac{d}{2}$ = radius of connecting leg and

e = holding width.

To physically hold the ball head in the socket, the holding width 'e' should be greater than zero. if θ_{bs} denotes the rotation angle of the joint on the XZ plane, rotational limits of joint are given by [3]

$$\pi - \left\{\sin^{-1}\left(\frac{d}{2\,r_b}\right) + \sin^{-1}\left(\frac{e}{r_b}\right)\right\} \geq \theta_{bs} \geq \left\{\sin^{-1}\left(\frac{d}{2\,r_b}\right) + \sin^{-1}\left(\frac{e}{r_b}\right)\right\} \quad (4.10)$$

A little consideration will show that it is quite difficult to fabricate a ball-and-socket joint which has ± 80° rotation about two normal axes. Since the joint strength was not a major requirement in the present design, the joint has been replaced by a three-axis universal type joint [Fig. 4.4(b)]. By this choice we have avoided the limitation on rotations customarily encountered with ball joints.

4.3.3 INTERFERENCES IN PRESENT DESIGN

An assembly of three-axis joint (S-joint) and the upper support bar has been shown in Fig. 4.4(b). The upper support bar is L-shaped. If

h_uj represents constant height of the center of the S-joint and

r', r are the apparent and actual radii of the platform respectively.

$h\_uj \cong z_{min}$,

$$\left[r' - r\right] < h_{uj} \qquad (4.11)$$

The choice of non zero $\left[r' - r\right]$ for fabricational convenience necessiates the height h_{uj} This height h_{uj}, which ensures interference free movements for negative values of z, could cause actuator interference for extreme positive values of z (generally, if α and β exceed $\frac{\pi}{3}$). This could have been avoided if

(i) the shape of the upper support bar is curved instead of L-shaped or

(ii) $\left[r' - r\right] = 0$, $h_{uj} \cong 0$ i.e. the center of the S-joint and ULA have common axis [see Fig. 1.4].

It is comparatively difficult to fabricate such a link and joint combinations. Furthermore, it is highly difficult to realize a zero interference SPM even with the modifications (i) and (ii). Thus, as pointed out before, the present design of SPM has link interferences but on negligible scale.

4.4 WORKSPACE VOLUME CONSIDERATIONS

The work envelope also known as the robot operating envelope is the set of points representing maximum extension or reach of the robot tool in all directions. Reachable workspace is the space enclosed within this envelope. This can be divided further into following three groups:

(a) dexterous workspace (primary),

(b) secondary workspace,

(c) controllably dexterous workspace (CDW).

The dexterous workspace is defined as the set of points Q in the workspace for which the end effector can assume all attitudes

when its reference point is coincident with Q. In other words, for any reference attitude of the end effector it can completely rotate about any arbitrary line through Q. This called the primary workspace while the other points in the reachable workspace is termed the secondary workspace. The controllably dexterous workspace is a sub set of the dexterous workspace where, for the reference point fixed at any point Q, the end effector can rotate completely about any arbitrary line through Q executing continucus and smooth motion. Points of singularity for example may belong to the dextrous workspace but not in the controllable workspace.

A 6-R PUMA type robot whose pitch, yaw and approach motions [n, s, a] are identified with the last three joints or a three degrees-of-freedom planar parallel manipulator [Fig 1.3] whose base joints are powered by rotary actuators or two cooperating 6-R manipulators, do have considerably large dexterous workspace. But in an SPM it is difficult to realize a large dexterous workspace for two primary reasons.

- Firstly, as an approximation if we consider the dexterous workspace to be primarily a function of range of orientation of an SPM. This calls for a very small value of $\left[\frac{r}{\delta}\right]$. Achieving that we have seen is very constraining in the present design.

- Secondly, following the above proposition, even if we lower the value of $\left[\frac{r}{\delta}\right]$ full range of orientation of the platform is not guaranteed. The limitation on the rotatability of S-joints or actuator interferences hinder full rotation. The only way around this is completely different 'system' design which is outside the scope of the present work.

In all future discussions, workspace means the regions of

the three-dimensional Cartesian space that are reachable by the manipulator with a given orientation of the platform. In this way, workspace becomes a function of the orientation at which the platform is being held at. The orientation aspect has been addressed by minimizing the chances of interferences by having a reasonably large value of r.

4.4.1 WORKSPACE FORMULATION USING INVERSE KINEMATICS

The inverse kinematics equations (2.7) and (2.11) can be expressed in a general form as given below :

(h_usb *has not been considered*)

for i = 1, 2, 3

$$Li^2 = \left(x - xc_i\right)^2 + \left(y - yc_i\right)^2 + \left(z - zc_i\right)^2, \qquad (4.12.1)$$

$$Di^2 = K_1 + K_2 \left(\frac{z - zc_i}{Li}\right), \qquad (4.12.2)$$

while

$Li_{min} \leq Li \leq Li_{max}$ and

$Di_{min} \leq Di \leq Di_{max}$.

$[xc_i, yc_i, zc_i]^T$ represents the displacement of i^{th} corner due to orientation of the platform in the Fixed Reference Coordinate system and is given by

$$\begin{bmatrix} xc_i \\ yc_i \\ zc_i \end{bmatrix} = \begin{bmatrix} l_{mean} \cos \xi_i - fx_i \\ l_{mean} \sin \xi_i - fy_i \\ - fz_i \end{bmatrix} \qquad (4.12.3)$$

where

ξ_i = initial angle of ULA to x_v axis (constant).

$$\xi_1 = \pi,$$

$$\xi_2 = \frac{\pi}{3},$$

$$\xi_3 = \frac{5\pi}{3}.$$

$[fx_i, fy_i, fz_i]^T$ are given by (2.9) or (2.13).

For a given orientation of the platform and for a given length of ULA, the equations (4.12.1) represent spheres whose centers are given by $[xc_i, yc_i, zc_i]^T$. For a given value of z_p and calculated value of length of the ULA, the LLA length Di can be varied to keep z_p constant.

Given the orientation of the platform, workspace of an SPM is the intersection of the following six spherical segments :

For i = 1, 2, 3

$$\left(Li_{max}\right)^2 = \left(x - xc_i\right)^2 + \left(y - yc_i\right)^2 + \left(z - zc_i\right)^2, \qquad (4.13.1)$$

$$\left(Li_{min}\right)^2 = \left(x - xc_i\right)^2 + \left(y - yc_i\right)^2 + \left(z - zc_i\right)^2, \qquad (4.13.2)$$

while

$Di_{min} \leq Di \leq Di_{max}$.

The lengths of ULA represent the radii of corresponding spheres. Additionally center of the sphere in FRC depends on the orientation of the platform, and does not necessarily coincide with the center of the upper RR-joints. If z_p is also kept constant, the length of LLA is determined by the length of the corresponding ULA.

4.4.2 GENERATING WORKSPACE BOUNDARY

From design standpoint, we are not interested in computing the exact workspace volume. We seek a technique to associate numbers with a given configuration so that comparisons can be

made. We have decided to compute the workspace volume as the set of points which can be reached by the center of the platform with the platform being maintained parallel to the base and not undergoing any twist during the translation. We feel this is an adequate measure of the workspace from the point of view of designing an SPM. Hence, the set of points reachable by the platform center by keeping orientation an identity has been considered as workspace boundary of SPM.

For $[\underset{\sim}{n}, \underset{\sim}{s}, \underset{\sim}{a}] = I$, $fx_i = 0$, $fy_i = 0$ and $fz_i = 0$. Hence the inverse kinematic equations will simplify to the form of (4.5.1) and (4.5.2). A numerical algorithm for detecting the workspace boundary on the XY-plane is presented as follows :

(i) For a given value of z_p, α, β and γ (or direction cosines of platform-fixed coordinate), find the extreme values of say x_p for $y_p = 0$ (i.e., $\left(x_p\right)_{min}$ and $\left(x_p\right)_{max}$) using equations (2.8) and (2.11) with actuator constraints viz.,

$$Li_{min} \leq Li \leq Li_{max} \text{ and}$$

$$Di_{min} \leq Di \leq Di_{max}.$$

(ii) Find extreme values of y_p for different values of x_p while $\left(x_p\right)_{min} < x_p < \left(x_p\right)_{max}$ with actuator constraints.

(iii) Outline the workspace boundary from the recorded extremes.

The same technique has been employed in generating XZ and YZ sections of the workspace by keeping y_p and x_p respectively as constants. Moreover, by keeping the orientation as an identity, equations (2.8) and (2.11) can be directly replaced by (4.5.1) and (4.5.2), respectively. In our implementation, the equations (4.5.1) and (4.5.2) have been used in generating the workspace boundries and few such results have been shown in figures 4.5(a), 4.5(b) and 4.5(c).

Fig. 4.5 (a) XY-section of workspace

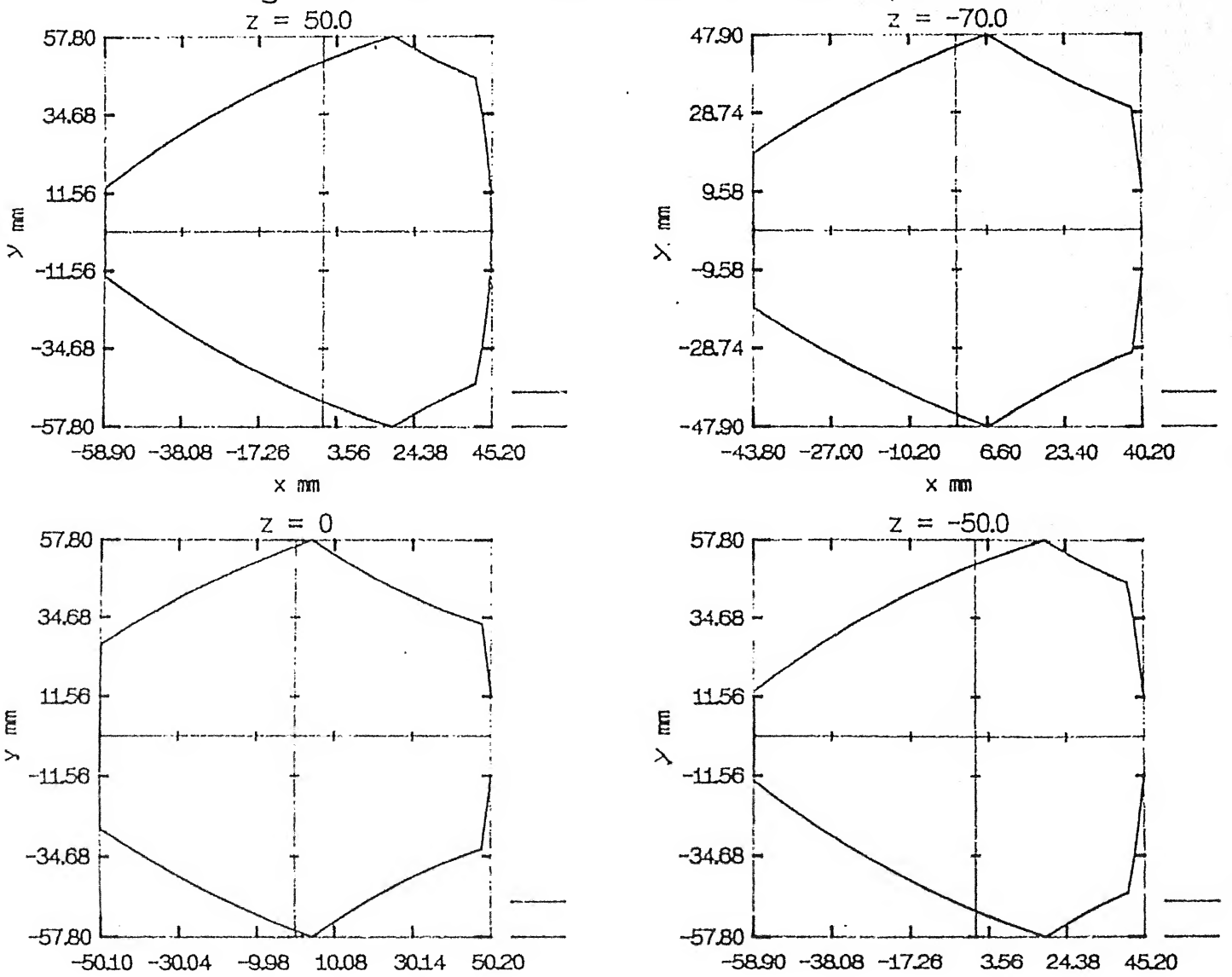

Fig. 4.5 (b) XZ-section of workspace

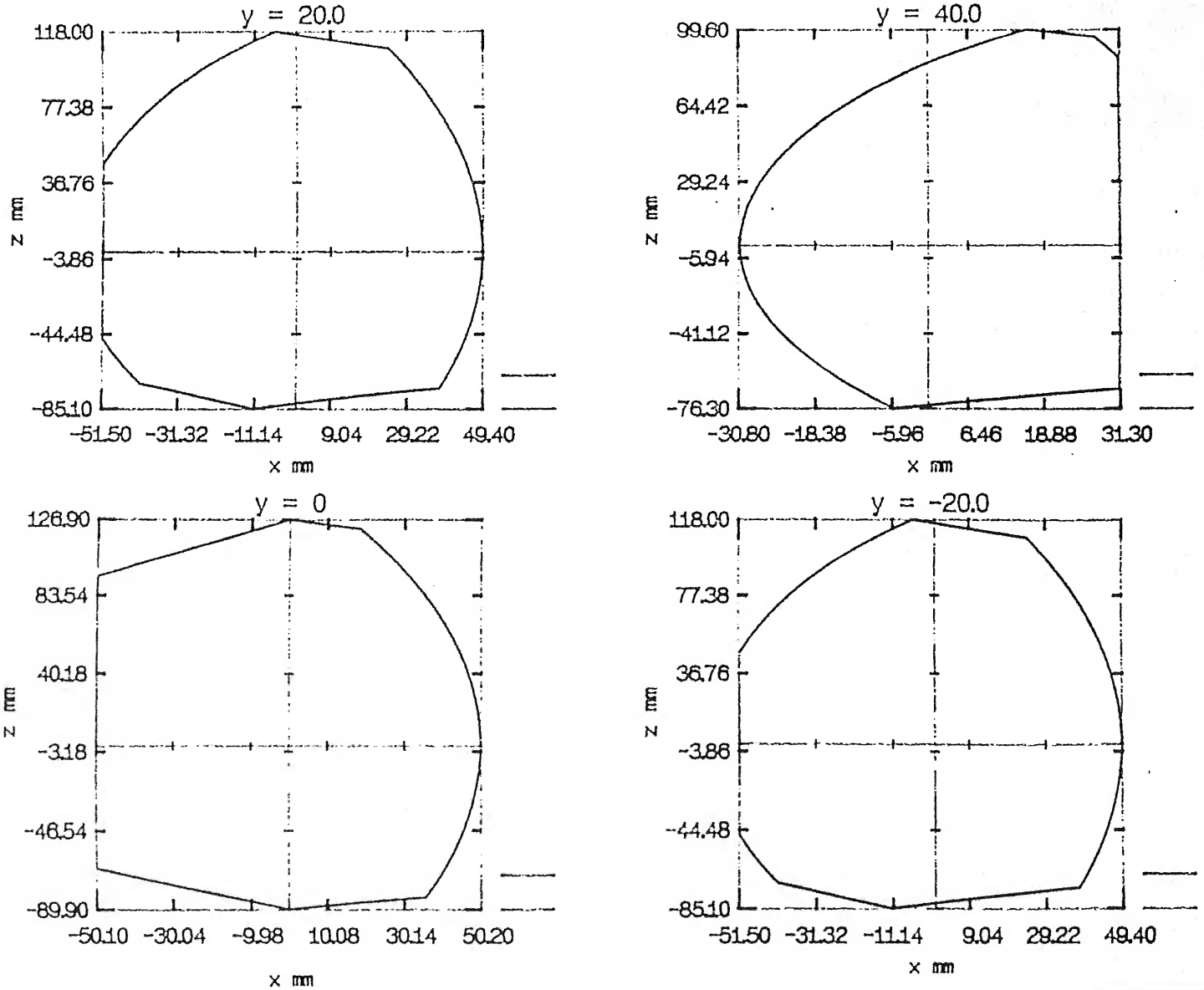

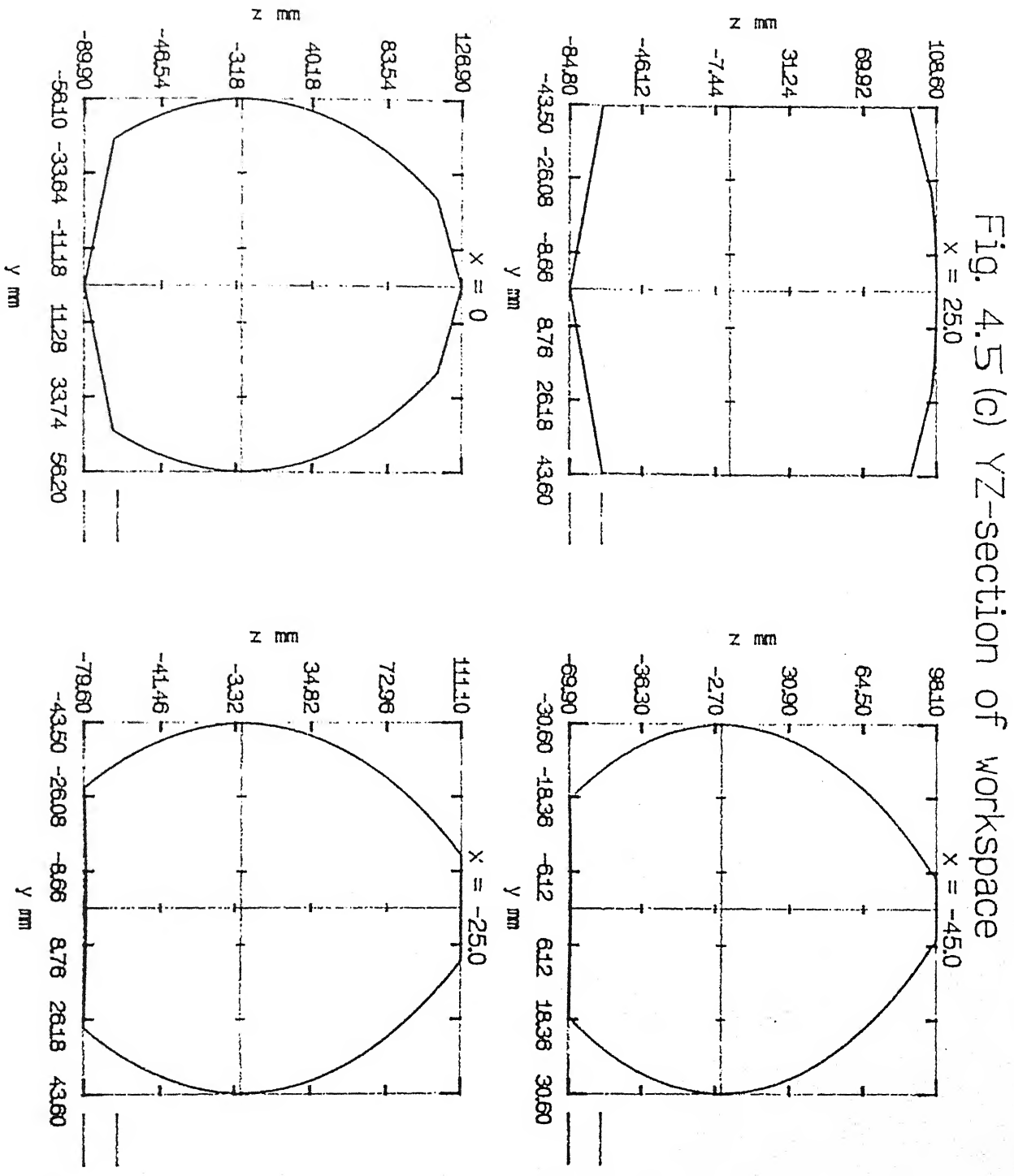

Fig. 4.5 (c) YZ-section of workspace

In general,for any given orientation of the platform, workspace boundary can be generated using the inverse kinematic equations. In the present case, since the rotation of the S-joints is not a limitation, no check of joint motion limitation during numerical iterations is needed.

4.5.3 COMPUTATION OF WORK VOLUME

Work volume in the present context is the volume of workspace generated by the previous algorithm. Once the boundary arcs have been generated, their point of intersection, center of curvature can be computed numerically and Gauss Divergence theorem can be used find the work area [6].

The method we employed here is as follows :

$$\left(\text{AREA}\right)_{z_p=\text{const}} = \frac{1}{2} \Sigma\, r_{wb}^{\,2}\, d\theta,$$

$$d\theta \to 0,$$

where

$$d\theta = \tan^{-1}\left(\frac{y_n}{x_n}\right) \sim \tan^{-1}\left(\frac{y_{n+1}}{x_{n+1}}\right)$$

(x_n, y_n), (x_{n+1}, y_{n+1}) being two close boundary points and

$$r_{wb} = \sqrt{x_n^2 + y_n^2} \quad . \tag{4.14}$$

The method we used is quite elementary and deviates from true Gauss Divergence theorem. It gives results accurate enough for comparative analysis.

Workspace volume can be determined by computing areas of series of parallel XY planes [see fig. 4.6] using the trapezoidal

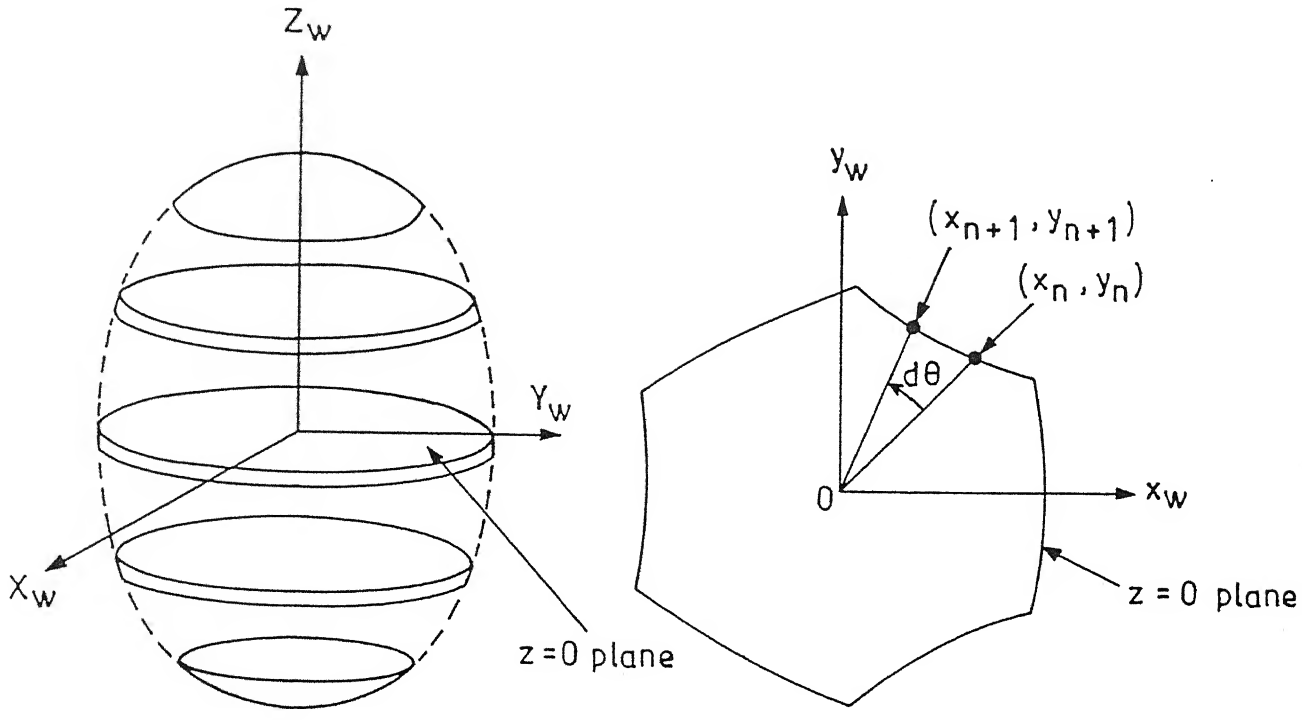

Fig. 4.6. Spatial representation of the workspace volume of an SPM for the reference orientation of the platform.

rule.

$$\text{WORKSPACE VOLUME} = \frac{1}{2} \sum_{z_{min}}^{z_{max}} \left\{ \left[\text{AREA}\right]_{z_n} + \left[\text{AREA}\right]_{z_{n+1}} \right\} dz \ ,$$

$$dz \to 0,$$

$$dz = z_{n+1} \sim z_n \ . \qquad (4.15)$$

4.4.4 EFFECT OF PLATFORM SIDE OR ULA MEAN LENGTH ON WORKSPACE VOLUME

Relationship between the support radius (R), mean length (l_{mean}) and platform radius (r) can be expressed as follows :

$$R^2 = l_{mean}^2 + r^2$$

or

$$(support\text{-}side)^2 = (platform\text{-}side)^2 + 3\, l_{mean}^2. \qquad (4.16.1)$$

Also,

$$Li_{max} = l_{mean} + \delta \quad \text{and}$$

$$Li_{min} = l_{mean} - \delta. \qquad (4.16.2)$$

Assuming R as constant, workspace volume of SPM can be computed for different values of l_{mean} (or platform side) using (4.16.1), (4.16.2) and (4.15). Figures 4.7(a) and 4.7(b) are identical except that the abscissa has been interpreted as ULA mean length and platform side respectively. R is the same for both the cases.

Workspace volume of an SPM, being predominantly a function of z_{range}, increases with increase in mean length. Since R has been assumed as constant, workspace volume increases with

application, just the workspace volume criterion can not provide a complete basis for deciding the platform side and mean length.

In the present design, r = 75 mm, R = 212 mm, l_{mean} = 198 mm gives an approximate workspace volume of 1.4 X 10^6 mm^3.

4.5 COMPACTNESS OF SPM AS A DESIGN CONSIDERATION

The space occupied by an SPM does have significance when it is to be designed for any specific practical application (e.g., as a fixture in an assembly line or transfer machines). If we define this space as manipulator occupied space, volume of this space can be approximated to volume of a cylinder of height equal to the height of support leg and radius equal to the radius of support structure (R). Given the two SPM's which have identical dynamic performance, intelligence etc., a compactness index expressed as workspace volume as a percentage of manipulator occupied space volume could be one of the measures of comparison.

Workspace volume of an SPM as we discussed before, is dependent on the stroke of actuators as well as mean length of ULA. The manipulator occupied space is mainly dependent on the type of support structure used. The size of support structure is decided by the l_{mean}, δ, r and h_{spp}. Hence, the right choice and design of the support structure is equally important as ensuring a large dexterous workspace, in achieving compactness in SPM design. As discussed in section 4.3.1, case(iii) [see Fig. 4.2] was the proper choice in the present case.

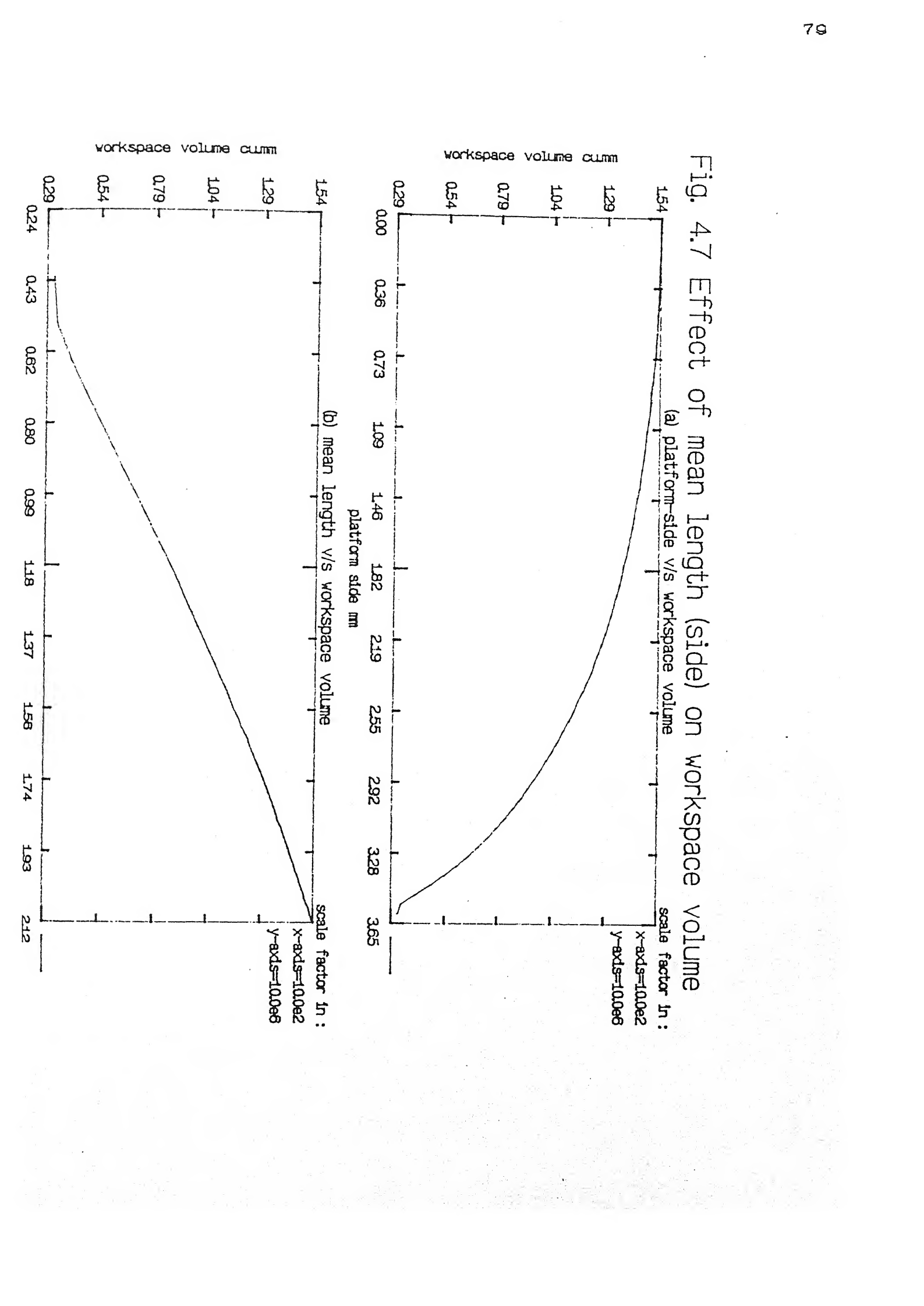

Fig. 4.7 Effect of mean length (side) on workspace volume

4.6 DISCUSSIONS

Figure 4.8 shows an SPM, developed in accordance with the considerations presented in this chapter. Major dimensions of the set-up and specifications have been listed in appendix II.

In the design of an SPM from kinematic view point, the link interference and the manipulator workspace are the major considerations. The design of support or foundation has direct bearing in reducing the manipulator occupied space and hence, its choice and design needs considerable attention.

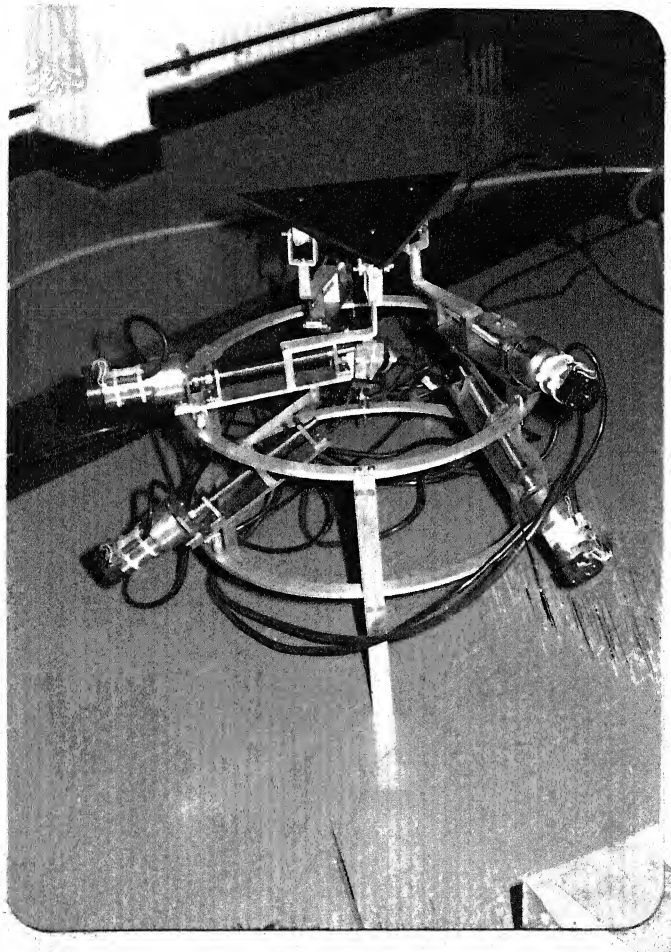

Fig. 4.8 Stewart Platform Manipulator.

CHAPTER 5

CONCLUSIONS

The Stewart Platform Manipulator, we considered here is the one proposed by Stewart,D [1]. There is no such comprehensive literature related to the design of this particular configuration.

The problem of position kinematics has been used in analyzing the geometry of the manipulator. This notion has been extended to the design of the manipulator from kinematic view point. The strength requirements of various links and dynamics of actuation have not been considered, which are the major drawbacks of the present work.

The problem of actuator interference has been nearly eleminated in the present design. The workspace of the manipulator as we analyzed is dependent on the size of the manipulator and its end effector. The range of orientation desired and the link interferences are the considerations, that could decide the size of the platform as well as the size of the manipulator.

The notions of dexterous workspace and controllably dexterous workspace along with singularity considerations have not been used in the present design. They could be considered in future redesigns or if high performance designs are needed.

REFERENCES

1. Stewart, D., 1965, " A platform with six degrees of freedom," *Proceedings of Institution of Mechanical Engineers*, vol.180, No.5, pp.371-378.

2. Hirochika Inoue, Yuji Tsusaka and Takeshi Fukuizumi, " Parallel manipulator," *The third Interational Symposium on Robotics Research*, pp.321-327.

3. Yang, D.C.H., and Lee, T.W., 1984, " Feasibility study of a platform type of Robotic manipulators from a kinematic view point," *ASME Journal of Mechanisms, Transmissions, and Automation in Design,"* vol.106, No.2, pp.191-198.

4. Gosselin, C., and Angeles.J., 1988, " The optimum kinematic design of a planar three degree-of-freedom parallel manipulator," *ASME Journal of Mechanisms, Transmissions and Automation in Design,"* vol.110, No.1, pp.35-41.

5. Gosselin, C., and Angeles.J., 1990, " Kinematic inversion of parallel manipulators in the presence of incompletely specified tasks, " *ASME Journal of Mechanisms, Transmissions, and Automation in Design,"* vol.112, No.4, pp.494-500.

6. Gosselin, C.,"Determination of the workspace of 6-DOF parallel manipulators, "*ASME Journal of Mechanisms, Transmissions, and Automation in Design,"* vol.112, No.3, pp.331-336.

7. Hunt, K.H., and Primrose, E.J.F., 1993, " Assembly configurations of some in-parallel-actuated manipulators," *Mechanical Machine Theory*, Vol.28, pp.31-42.

8. Nanua, P., and Waldron, K.J., 1989, " Direct kinematic solution of a Stewart platform," *Proceedings, IEEE International Conference on Robotics and Automation*, vol.1, pp.431-437.

9. Lin, W., Griffis, M., and Duffy, J., 1992, " Forward displacement analysis of the 4-4 Stewart platforms," *ASME Journal of Mechanical Design*, Vol.114, No.3, pp.444-450.

10. Parenti-Castelli, V., and Innocenti, C., 1992, " Forward displacement analysis of parallel mechanisms : closed form solution of PRR-3S and PPR-3S structures," *ASME Journal of Mechanical Design*, Vol.114, No.1, pp.68-73.

11. Kumar.V., 1992, " Characterization of workspaces of parallel manipulators," *ASME Journal of Mechanical Design*, Vol.114, No. 3, pp.368-374.

12. Shimon Y. NOF. (editor), 1985, "*Handbook of Industrial Robots*," John Wiley & Sons, Inc.

13. Ghosh, A., Mallik, A.K., 1976, " *Theory of mechanisms and machines*," East West press, New Delhi.

14. Brice Carnahan, Luther, A.A., James, O.Wikes., 1969, " *Applied Numerical Methods*," John Willey and Sons, Inc.

APPENDIX I

LIST OF COEFFICIENTS IN DIRECT POSITION KINEMATICS

The coefficients appearing in (3.3.1), (3.3.2) and (3.3.3) are listed below :

$$A1 = B1 = -2\ L1\ L2 \cos\theta_{21} \cos\theta_{22},$$

$$A2 = B2 = -2\ L2\ L3 \cos\theta_{22} \cos\theta_{23},$$

$$A3 = B3 = -2\ L3\ L1 \cos\theta_{23} \cos\theta_{21},$$

$$C1 = 2\ R\ L1 \cos\theta_{21} \left(\cos\phi_1 - \cos\phi_2 \right),$$

$$C2 = 2\ R\ L2 \cos\theta_{22} \left(\cos\phi_2 - \cos\phi_3 \right),$$

$$C3 = 2\ R\ L3 \cos\theta_{23} \left(\cos\phi_3 - \cos\phi_1 \right),$$

$$E1 = 2\ R\ L1 \cos\theta_{21} \left(\sin\phi_1 - \sin\phi_2 \right),$$

$$E2 = 2\ R\ L2 \cos\theta_{22} \left(\sin\phi_2 - \sin\phi_3 \right),$$

$$E3 = 2\ R\ L3 \cos\theta_{23} \left(\sin\phi_3 - \sin\phi_1 \right),$$

$$F1 = 2\ R\ L2 \cos\theta_{22} \left(\cos\phi_2 - \cos\phi_1 \right),$$

$$F2 = 2\ R\ L3 \cos\theta_{23} \left(\cos\phi_3 - \cos\phi_2 \right),$$

$$F3 = 2\ R\ L1 \cos\theta_{21} \left(\cos\phi_1 - \cos\phi_3 \right),$$

$$H1 = 2\ R\ L2 \cos\theta_{22} \left(\sin\phi_2 - \sin\phi_1 \right),$$

$$H2 = 2\ R\ L3 \cos\theta_{23} \left[\sin\phi_3 - \sin\phi_2 \right],$$

$$H3 = 2\ R\ L1 \cos\theta_{21} \left[\sin\phi_1 - \sin\phi_3 \right],$$

$$G1 = \left[L1 \cos\theta_{21} \right]^2 + \left[L2 \cos\theta_{22} \right]^2 + \left[L1 \sin\theta_{21} - L2 \sin\theta_{22} \right]^2 +$$

$$\left[R \cos\phi_1 - R \cos\phi_2 \right]^2 + \left[R \sin\phi_1 - R \sin\phi_2 \right]^2 - 3\ r^2 ,$$

$$G2 = \left[L2 \cos\theta_{22} \right]^2 + \left[L3 \cos\theta_{23} \right]^2 + \left[L2 \sin\theta_{22} - L3 \sin\theta_{23} \right]^2 +$$

$$\left[R \cos\phi_2 - R \cos\phi_3 \right]^2 + \left[R \sin\phi_2 - R \sin\phi_3 \right]^2 - 3\ r^2 ,$$

$$G3 = \left[L3 \cos\theta_{23} \right]^2 + \left[L1 \cos\theta_{21} \right]^2 + \left[L3 \sin\theta_{23} - L1 \sin\theta_{21} \right]^2 +$$

$$\left[R \cos\phi_3 - R \cos\phi_1 \right]^2 + \left[R \sin\phi_3 - R \sin\phi_1 \right]^2 - 3\ r^2 .$$

APPENDIX II

SPECIFICATIONS OF STEWART PLATFORM MANIPULATOR

Lead-screw : M12 X 1.75

l_ueb : 111 mm

h_ueb : 132 mm

δ : 50 mm

L_{max} : 248 mm

l_{mean} : 198 mm

L_{min} : 148 mm

l_leb : 99 mm

h_leb : 72 mm

D_{max} : 236 mm

dmean : 186 mm

D_{min} : 136 mm

r' : 150 mm

r : 75 mm

R : 212 mm

h_epp : 150 mm

d_hg : 132 mm

$(\theta_{2i})_{range}$: 56°

$(x)_{range}$: 100 mm

$(y)_{range}$: 115 mm

$(z)_{range}$: 215 mm

$(\alpha)_{range}$: 170°

$(\beta)_{range}$: 170°

$(\gamma)_{range}$: 85°

Date Slip

This book is to be returned on the date last stamped.
